DET NORSKE VERITAS
INDUSTRY AS

VERITEC

TECHNICAL REPORT

190
AH

Veritasveien 1,
N-1322 HØVIK
Telephone (+47) 67 57 72 50
Facsimile (+47) 67 57 74 74
Registration No. 834 763 052

Date:	Div.-Dept.:	
4 August 1994	T&I-212	
Approved by: Einar Tore Moe, Head of Section for Structural Connections		
Client, Sponsor: Exxon, Amoco, Elf, Mobil, Conoco and MMS	Client ref.:	Project No.: 161119

Summary:

Early age cycling, fatigue and static strength tests have been performed on grouted connections to determine the fatigue strength of grouted connections with large and densely spaced shear keys as well as the effect or early age cycling. Large and densely spaced shear keys lead to reduced shear strength. Too closely spaced shear keys may cause early age cycling to produce a very significant reduction of strength. This reduction in strength depends on the trajectory of the disturbed zone produced by the early age cycling. A straight trajectory causes significant strength reduction while an undulating trajectory has no significant impact. The shape of the trajectory depends on the shear key spacing. It has also been found that fatigue tests performed in straight force control may tend to produce results which are not representative of grouted connections in offshore structures.

Report No.:	Subject Group:	
94-3243	D8, P3	
Report title: Factors of Safety for Grouted Connection Phase II the Impact of Cyclic Load on Connections with High H/S Values		
Work carried out by: Monica Skjolde		
Work verified by: for Arne Sele		
Date of last rev.:	Rev.No.:	Number of Pages: 71

Indexing terms

TESTS
JOINTS
CYCLIC LOADS
FATIGUE

[X] No distribution without permission from the responsible department/project

[ ] Limited distribution within DNV Industry

[ ] Unrestricted distribution

Table of Contents:

		Page
1	SUMMARY AND CONCLUSIONS	3
2	INTRODUCTION	5
3	PREVIOUS TESTS ON RECORD	6
4	TEST PROCEDURE	12
4.1	Preparation of test specimen	12
4.2	Early age cycling	20
4.3	Fatigue Testing	21
4.4	Summary of specimens	22
5	TEST EXECUTION	25
5.1	Specimen no 1	25
5.2	Specimen no 2	25
5.3	Specimen no 3	25
5.4	Specimen no 4	31
5.5	Specimen no 5	31
5.6	Specimen no 6	31
5.7	Specimen no 7	43
5.8	Specimen no 8	43
5.9	Specimen no 9	43
5.10	Specimen no 10	47
5.11	Test results received from the UK project	51
6	EVALUATION OF THE TEST RESULTS:	60
6.1	Specimen no 1	60
6.2	Specimen no 3	60
6.3	Plain fatigue tests	60
6.4	Tests with early age cycling and fatigue	65
6.5	Tests with early age cycling only	67
7	REFERENCES	68

APPENDIX A - Specification of oil well G cement

1 SUMMARY AND CONCLUSIONS

The aim of the present work is to assess the behaviour of grouted pile-sleeve connections exposed to cyclic loading. The work is performed in order to provide a better understanding of the effects of early age cycling as well as cyclic loads throughout the lifetime of the connection.

In order to perform this work a total of ten tests have been executed at the Det Norske Veritas laboratories at Høvik. The conclusions drawn are based on the results of these ten tests supplemented by ten tests performed in the UK /10/ and the results of 21 previous tests performed by DnV in 1984 as well as 10 tests performed by Wimpey in 1982, ref./8/ and /7/. The present and the previous tests refereed to herein have mostly been performed with ration of maximum to minimum load of R= -1. The use of this test condition represents a conservative approach to design.

Three of the specimens have been exposed to fatigue testing after the grout having reached a desired strength. These tests show that the fatigue strength expressed as fraction of the static strength reduces where higher and more densely spaced shear keys are used.

Four specimens have been exposed to cyclic displacement during the setting of the grout and the early stage of curing. Fatigue testing was subsequently performed when the desired grout strength was reached. Such early age cycling has a severe effect on the strength of specimens with closely spaced shear keys. For specimens with more widely spaced shear keys the impacts of early age cycling is very much reduced.

Two specimens have been sectioned after early age cycling. They reveal that a very narrow band of disturbed grout with severely reduced strength forms over the entire length of the specimens. For closely spaced shear keys this band forms a straight line through the grout accounting for the strength reduction observed. For more widely spaced shear keys the band of disturbed grout undulates between the top of the shear keys and the grout to steel interface. This still allows the wedging action of the shear keys to be mobilized and accounts for the fact there is little impairment of strength where shear keys are widely spaced.

One specimen has been tested for static strength as a reference to improve the accuracy of the estimated static strength.

Observations during testing strongly indicate that execution of such tests in plain force control is likely to have been too onerous a test condition. Test results obtained to date may to a greater or lesser degree underestimate the actual strength obtainable in service. Future tests must incorporate controls which limit displacement rates to a realistic level.

2 INTRODUCTION

Phase II of the project "Factors of Safety for Grouted Connections" follows on from the first phase. In phase I the factors of safety required to give grouted connections the same level of reliability as achieved for other structural components were assessed. With these factors of safety which have been adopted in the DnV code for fixed offshore structures it was recognised that it was necessary to address the effects of cyclic load. Two effects are associated with cyclic load. These are fatigue and early age cycling.

The test results which are available to date all have been performed on specimens with shear key height to spacing ratios (h/s) of about 0.01. It was necessary to verify what the influence of cyclic loading would be throughout the complete design range. As work is in progress in Britain on specimens with very closely spaced weld beads this project has concentrated on specimens with larger and more widely spaced weld beads. The latter configuration leads to connections with greater static strength.

From previous work it has been established that fatigue strength in terms of peak stress is related to ultimate strength. In the interest of economy and efficiency all testing is therefor performed on one specimen configuration which is reused for all the strength tests. As it is the same specimen which is reused this also provides for greater repeatability as all geometrical parameters are identical.

In previous tests at $h/s = 0.01$ no influence of early age cycling was detectable. At the outset of this work it was therefor necessary to provide for the two alternative cases that fatigue with early age cycling either was or was not more critical than fatigue without early age cycling. It was therefor provided that the steering committee would review test results as work progressed. Subsequent tests were authorised based on the findings from the preceding ones such that an optimum allocation of specimens between those with and those without early age cycling could be achieved.

3 PREVIOUS TESTS ON RECORD

In the early 1980's fatigue testing of grouted connections was performed in a joint industry funded project organised by DnV and one organised by the Department of Energy in the U.K. The details of the DnV specimens are given in table 3.1 and the test results in table 3.2. The details of the U.K tests are given in table 3.3. Both sets of tests had shear key height to spacing ratios of close to 0.01.

The test results from both projects are shown in Figure 3.1. Here the results are plotted in terms of the ratio of peak stress to peak strength versus the logarithm of the number of cycles for various ratios of maximum to minimum stress (R). This type of plot has been used in the treatment of fatigue of grouted connections in previous work. Plotting on a log-log scale is more conventional in fatigue work. This is done in Fig. 3.2. It is seen that cyclic load does not have very significant impact for amplitude ratios ranging from R = 0.3 through 0 to -0.5. However, for R = -1 there is a more significant impact. This is still not sufficient to be critical to structures exposed to environmental loading.

These results support the postulation by R. Harwood of Shell UK that no fatigue damage will accrue in grouted connections which are not loaded and also reverse loaded in excess of the corresponding plain connection capacity.

All tests being performed in Britain have conservatively adopted R = -1, as is the case also for this project. The previous tests with R = -1 are shown separately in Figure 3.2. This is the principal reference for the evaluation of the new data. The new data has shear key height to spacing ratios ranging from 0.05 to 0.08.

FATIGUE TESTING OF GROUTED CONNECTIONS

Table 3.1 Geometry of shear key specimens, PP4 of DNV project

SPECIMEN	PILE		SLEEVE		GROUT		OD/T-RATIO			GROUT ANNULUS			PILE - SHEAR KEYS				
	OD	T	OD	T	OD	T	PILE	SLEEVE	GROUT	LENGTH, L	BOND AREA	L/OD_{pile}	HEIGHT, H	SPACINGS, S	H/S	OD_{pile}/S	H/OD_{pile}
4 A 1	353,8	13,7	406,0	12,6	380,8	13,5	25,8	32,2	28,2	711	790162	2,01	2,20	340	0,0065	1,040	0,0062
4 A 2	357,0	13,3	406,0	12,8	380,5	11,8	26,8	31,7	32,2	715	801907	2,00	2,20	340	0,0065	1,050	0,0062
4 A 3	354,0	13,9	406,5	12,8	381,0	13,5	25,5	31 8	28,2	762	847438	2,15	2,10	340	0,0062	1,041	0,0059
4 B 1	354,3	13,0	407,3	13,3	380,8	13,3	27,3	30,7	28,6	735	817988	2,07	2,25	340	0,0066	1.042	0,0064
4 B 2	354,5	12,8	407,5	13,5	380,5	13,0	27,7	30,2	29,3	729	811883	2,06	2,25	340	0,0066	1.043	0,0063
4 B 3	355,7	13,0	406,5	12,7	381,1	12,7	27,4	32,0	30,0	730	815749	2,05	2,20	340	0,0065	1.046	0,0062
4 C 1	355,5	12,5	405,5	13,6	378,4	11,5	28,4	29,8	32,9	752	839302	2,12	2,25	340	0,0066	1.046	0,0063
4 C 2	356,0	13,8	406,0	13,5	379,1	11,6	25,8	30,1	32,7	705	788471	1,98	2,30	340	0,0068	1.047	0,0065
4 C 3	354,8	14,1	406,8	13,4	380,0	12,6	25,2	30,4	30,2	704	784594	1,98	1,90	340	0,0056	1.043	0,0054
4 D 1	357,0	13,0	405,7	12,5	380,7	11,9	27,5	32,5	32,0	714	800786	2,00	2,25	340	0,0066	1.050	0,0063
4 D 2	358,2	13,2	408,8	12,3	384,2	13,0	27,1	33,2	29,6	730	821483	2,04	2,25	340	0,0066	1.054	0,0063
4 D 3	356,1	13,4	409,1	12,9	383,3	13,6	26,6	31,7	28,2	733	820023	2,06	2,25	340	0,0066	1.047	0,0063
4 E 1	356,3	14,0	408,7	13,4	381,9	12,8	25,5	30,5	29,8	729	816006	2,05	2,25	340	0,0066	1.048	0,0063
4 E 2	357,7	13,0	409,0	13,2	382,6	12,5	27,5	31,0	30,6	727	816965	2,03	2,25	340	0,0066	1.052	0,0063
4 E 3	356,9	12,4	408,8	13,2	382,4	12,8	28,8	31,0	29,9	727	815137	2,04	2,25	340	0,0066	1.050	0,0063
4 F 1	354,5	13,0	406,3	13,5	379,3	12,4	27,3	30,1	30,7	697	776250	1,97	2,37	340	0,0070	1.043	0,0067
4 F 2	356,0	13,3	406,5	13,0	380,5	12,3	26,8	31,3	30,9	694	776000	1,95	2,28	340	0,0067	1.047	0,0064
4 F 3	356,3	13,5	406,5	13,0	380,5	12,1	26,4	31,3	31,4	696	779068	1,95	2,45	340	0,0072	1.048	0,0069
4 G 1	354,3	13,2	406,8	13,0	380,9	13,3	26,8	31,3	28,6	711	791278	2,01	2,28	340	0,0067	1.042	0,0064
4 G 2	357,0	13,7	406,0	13,0	380,0	11,5	26,1	31,2	33,0	708	794056	1,98	2,10	340	0,0062	1.050	0,0059
4 G 3	354,8	14,1	406,5	12,9	380,7	13,0	25,2	31,5	29,3	761	848119	2,14	2,30	340	0,0068	[illegible]	,0065

Measurements in mm

Conversion factor
1 mm = 0.0394 in

FATIGUE TESTING OF GROUTED CONNECTIONS

Table 3.2 Results from dynamic loading of specimens, PP4

SPECIMEN	CASTING	START TEST		END TEST		CORRECTED GROUT CUBE STRENGTH BY CORRELATION TESTS (N/mm²)			CALCULATED CAPASITY		APPLIED DYNAMIC LOAD					FAILURE			
	Date	Date	Age (days)	Date	Age (days)	Start	End	Average	$\tau_s = 0,47\sqrt{f_c}$ (N/mm²)	Load (KN)	Minimum (KN)	Minimum $\cdot\tau_s$	Maximum (KN)	Maximum $\cdot\tau_s$	Range $\cdot\tau_s$	Maximum number of Cycles	Displacement (mm)	$R = \tau_{min}/\tau_{max}$	Cycles for δ = 35 mm
4A1	01.12.81	26.01.82	57	30.01.82	61	38.6	41.7	40.1	2.98	2356	100	0,04	2000	0.85	0.81	345.699	70	0.05	345.287
4A2	07.01.82	04.02.82	28	05.02.82	29	43.1	42.8	42.9	3.09	2474	20	0.01	2300	0.93	0.92	3.950	66	0.01	3
4A3	07.01.82	08.02.82	32	09.02.82	33	44.1	-	44.1	2.97	2517	60	0.02	2080	0.83	0.81	56	46	0.02	25
4B1	20.10.82	10.02.83	112	11.02.83	113	43.8	43.8	43.8	3.11	2545	-630	-0.25	1880	0.74	0.99	79	35	-0.34	79
4B2	20.10.82	22.02.83	124	22.02.83	124	43.1	43.1	43.1	3.09	2505	-640	-0.26	1930	0.77	1.03	63	35	-0.34	63
4B3	20.10.82	07.03.83	137	07.03.83	137	43.4	43.4	43.4	3.10	2526	-670	-0.27	2020	0.80	1.07	96	35	-0.34	96
4C1	06.10.81	11.11.81	36	11.11.81	36	46.1	46.1	46.1	3.19	2679	-1160	-0.43	2270	0.85	1.28	250	43.5	-0.51	126
4C2	01.12.81	25.01.82	56	26.01.82	57	36.9	40.0	38.5	2.91	2298	-1120	-0.49	2200	0.96	1.45	250	77	-0.51	1
4C3	07.01.82	01.02.82	25	01.02.82	25	42.3	42.3	42.3	3.06	2398	-1100	-0.51	2250	0.94	1.45	96	66	-0.54	17
4D1	02.06.83	28.06.83	26	30.06.83	28	44.1	44.6	44.4	3.13	2507	530	0.21	2080	0.83	0.62	>160.000	2	0.25	>160.000
4D2	02.06.83	01.07.83	29	06.07.83	34	44.6	45.4	45.0	3.15	2589	726	0.28	2325	0.90	0.62	>160.000	8	0.31	>160.000
4D3	02.06.83	11.07.83	39	11.07.83	39	45.9	45.9	45.9	3.19	2612	716	0.27	2315	0.89	0.62	1.050	35	0.30	1.050
4E1	02.06.83	08.07.83	36	08.07.83	36	45.8	45.8	45.8	3.18	2595	-1844	-0.71	1884	0.73	1.44	20	17.5	-0.97	-
4E2	02.06.83	25.07.83	53	26.07.83	54	46.6	46.6	46.6	3.21	2622	-2000	-0.76	2000	0.76	1.52	5	35	-1.00	5
4E3	02.06.83	01.08.83	60	01.08.83	60	46.9	46.9	46.9	3.22	2622	-1717	-0.65	1717	0.65	1.30	12	35	-1.00	12
4F1	20.10.82	12.11.82	22	10.12.82	50	34.1	45.4	39.8	2.96	2300	20	0.01	1600	0.70	0.69	> $2\cdot10^6$	19.7	0.01	> $2\cdot10^6$
4F2	20.10.82	14.12.82	54	11.01.83	82	45.0	44.5	44.7	3.14	2440	20	0.01	1800	0.74	0.73	> $2\cdot10^6$	17	0.01	> $2\cdot10^6$
4F3	20.10.82	17.02.83	119	17.02.83	119	42.5	42.5	42.5	3.06	2387	0	0.00	2120	0.89	0.89	> 322	35	0.00	322
4G1	23.02.82	23.03.82	28	21.04.82	57	35.6	39.0	37.3	2.87	2271	30	0.01	1600	0.70	0.69	> $2\cdot10^6$	25	0.01	> $2\cdot10^6$
4G2	23.02.82	27.04.82	63	28.04.82	64	38.5	38.9	38.7	2.79	2219	30	0.01	1850	0.83	0.82	> 462	45	0.01	180
4G3	23.02.82	03.05.82	69	07.05.82	73	39.1	-	39.1	2.94	2493	50	0.02	1950	0.78	0.76	>300.000	43	0.03	373

Table 3.2 Results from Dynamic Loading of Specimens, PP4

NOTE: τ_s of specimen 4A3, 4C3 and 4G2 has been adjusted

Table 3.3 Geometry and results from tests carried out at Wimpey Laboratories, UK

Geometry : L/OD_{pile} = 1.0

	OD	t	D/t	h	s	h/s
Pile	324	10	32.4	1.3	108	0.012
Grout	356	16	22.3			
Sleeve	366	5	73.2	1.3	108	0.012

Measurements in mm. 1 mm = 0.0394 in

Sleeves of all 10 specimens were supported by 12 longitudinal stiffeners each. The geometry of each stiffener was 108 x 12 mm (4.3 x 0.5 in).

Test Results:

Specimen	Max. Applied Bond Stress	Stress Range	Number of Cycles LOGN
1	$0.59 \cdot \tau_s$	$1.18 \cdot \tau_s$	2.20
2	$0.57 \cdot \tau_s$	$1.14 \cdot \tau_s$	1.93
3	$0.52 \cdot \tau_s$	$1.04 \cdot \tau_s$	1.84
4	$0.47 \cdot \tau_s$	$0.94 \cdot \tau_s$	3.17
5	$0.47 \cdot \tau_s$	$0.94 \cdot \tau_s$	3.56
6	$0.53 \cdot \tau_s$	$1.06 \cdot \tau_s$	3.73
7	$0.40 \cdot \tau_s$	$0.80 \cdot \tau_s$	6.48
8	$0.36 \cdot \tau_s$	$0.72 \cdot \tau_s$	> 6.93
9	$0.27 \cdot \tau_s$	$0.54 \cdot \tau_s$	> 6.93
10	$0.23 \cdot \tau_s$	$0.46 \cdot \tau_s$	> 6.18

Figure 3.1

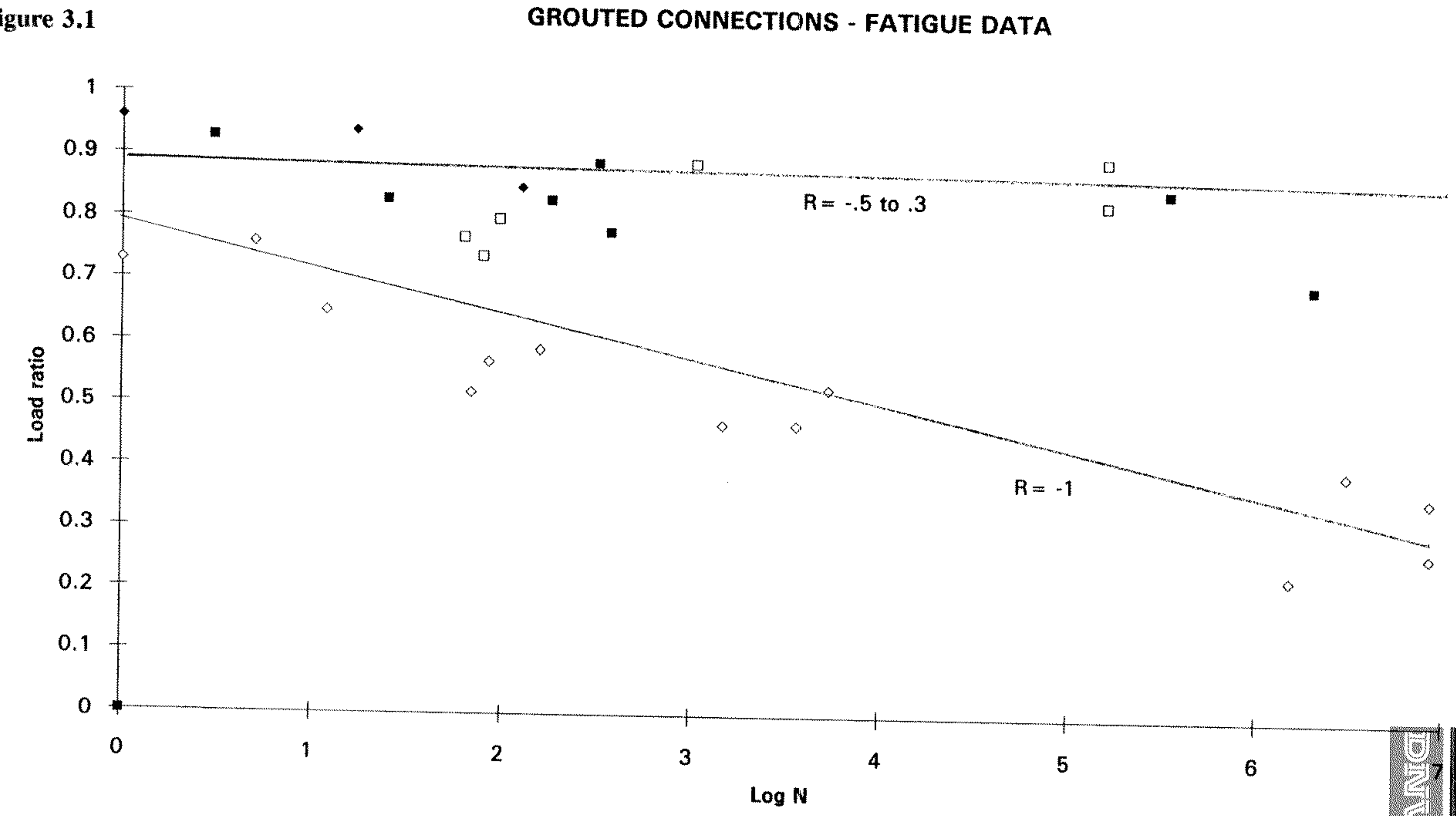
GROUTED CONNECTIONS - FATIGUE DATA
1
0.9
0.8
0.7
0.6
0.5
0.4
0.3
0.2
0.1
0
Load ratio
0
1
2
3
4
5
6
7
Log N
R = -.5 to .3
R = -1

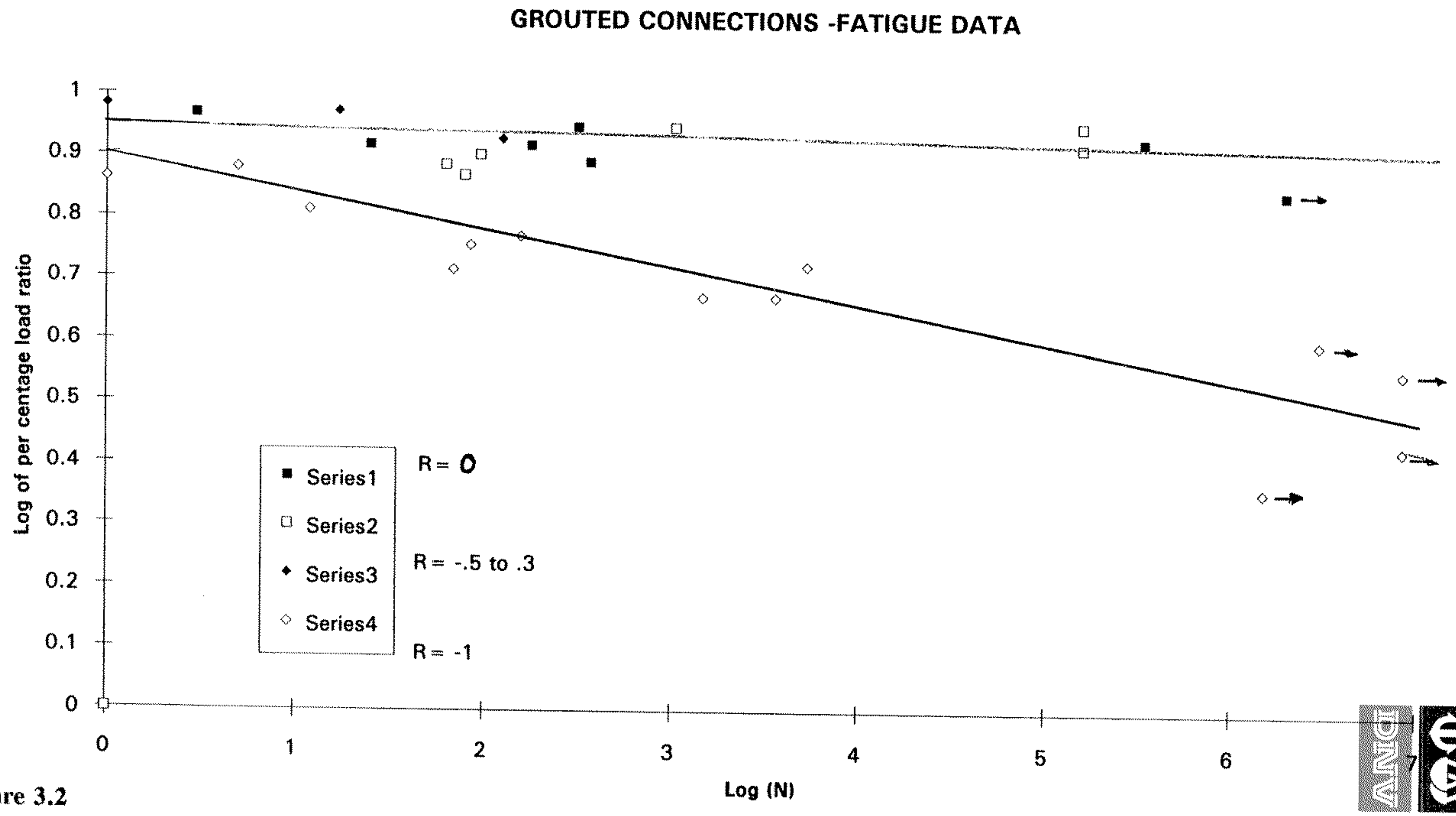
GROUTED CONNECTIONS -FATIGUE DATA
Log of per centage load ratio
1
0.9
0.8
0.7
0.6
0.5
0.4
0.3
0.2
0.1
0
0
1
2
3
4
5
6
7
Log (N)
Series1
Series2
Series3
Series4
R = 0
R = -.5 to .3
R = -1

Figure 3.2

4 TEST PROCEDURE

4.1 Preparation of test specimen

The same pile and sleeve are used in all tests. The geometrical data are as given below:

Pile:

D_p = 320.0 mm
t_p = 8.0 mm

Sleeve:

D_s = 395.0 mm
t_s = 8.0 mm

This gives a grout thickness in the test area of 29.5 mm.

Since the same test specimen is used for all tests, stiffeners were introduced to ensure that fatigue of the steel was avoided. The pile has sixteen longitudinal stiffeners on the inside. The sleeve has been strengthened with sixteen longitudinal stiffeners on the outside and inside, see figure 4.1.1. The effect of longitudinal stiffeners have been investigated earlier and found to have insignificant influence on the capacity of the grouted pile-sleeve connection, ref./ 9/.

The shear keys were manufactured as weld beads for all specimens except specimen no.1. On this specimen the shear keys were made by welding Ø = 10 mm round steel bars to the pile and sleeve surface.

TEST SPECIMEN CONFIGURATION

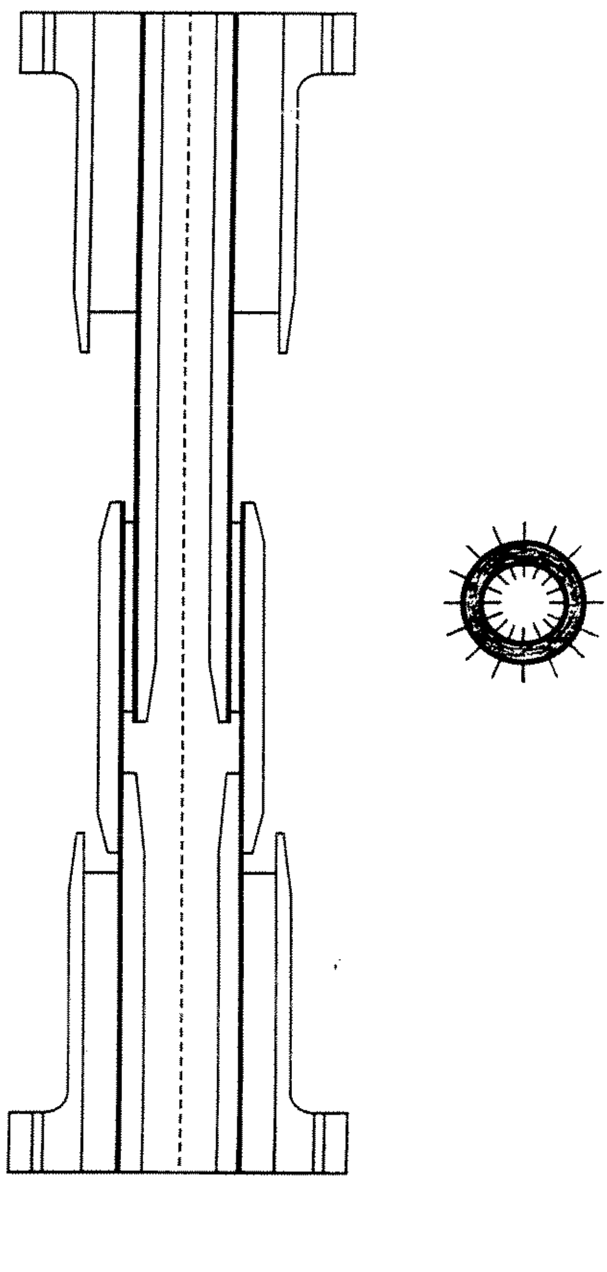

Figure 4.1.1 Test specimen configuration

The shear keys were attached to the outer surface of the pile and the inner surface of the sleeve. The shear keys are circumferential weld beads on bars with a nominal outstand between 2 and 10 mm. The shear key outstand and the shear key spacing varies; an overview of the combinations tested are given on page 23 in Table 4.4.1.

TEST 1

$S/\sqrt{R_p \cdot t_p} = 6$

$S = 215.0$ mm

$H = 10.0$ mm

$H/S = 0.046$

$L/D_p = 1.5$

TEST 2, 3, 4, 5 and 6

$S/\sqrt{R_p \cdot t_p} = 1$

$S = 36.0$ mm

$H = 3.0$ mm

$H/S = 0.083$

$L/D_p = 1.5$

TEST 7

$S/\sqrt{R_p \cdot t_p} = 1$

$S = 36.0$ mm

$H = 2.0$ mm

$H/S = 0.056$

$L/D_p = 1.5$

TEST 8, 9 and 10

$S/\sqrt{R_p \cdot t_p} = 3$

$S = 108.0$ mm

$H = 5.0$ mm

$H/S = 0.046$

$L/D_p = 1.5$

TEST 1

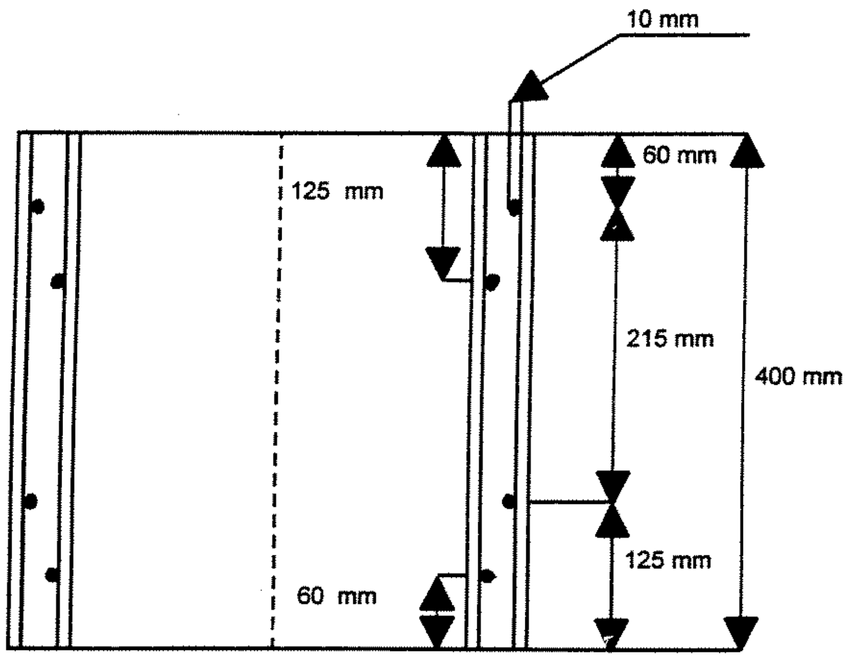

$S/\sqrt{R_p \cdot t_p} = 6$

$H/S = 0.05$

$L/D_p = 1.25$

TEST 2 , 3 , 4 , 5 and 6

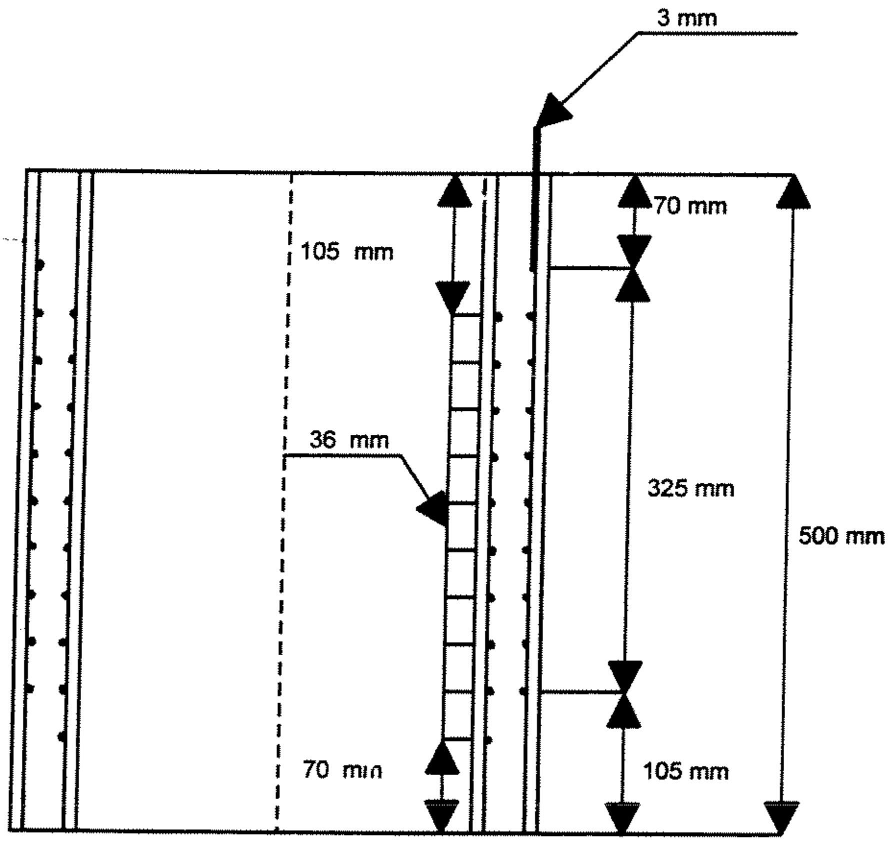

$$S/\sqrt{R_p \cdot t_p} = 1$$

$$H/S = 0.08$$

$$L/D_p = 1.5$$

TEST 7

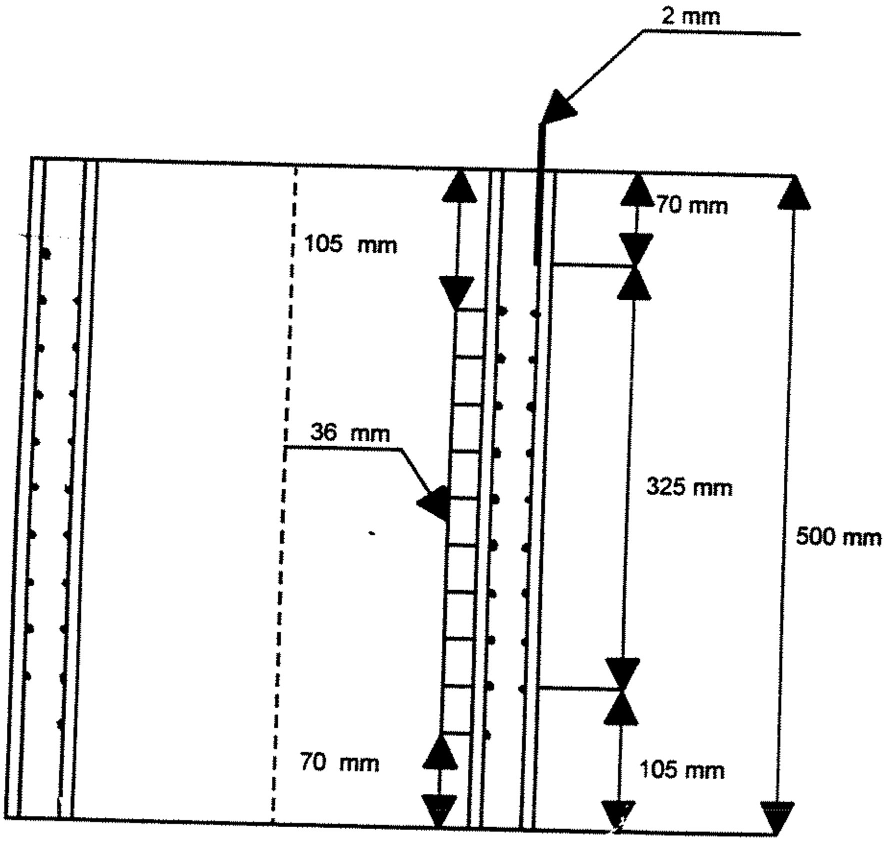

$$S/\sqrt{R_p \cdot t_p} = 1$$

$$H/S = 0.05$$

$$L/D_p = 1.5$$

4 August 1994, T&I-212 O:\BGF\161119\94-3243.REP

TEST 8, 9 and 10

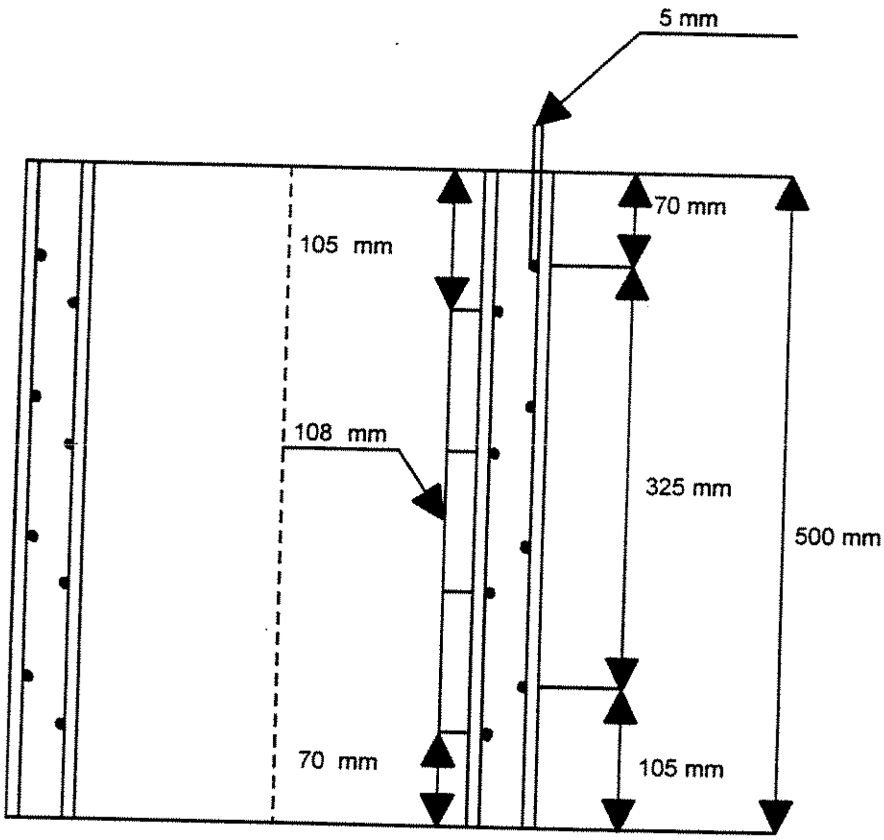

$$S/\sqrt{R_p \cdot t_p} = 3$$

$$H/S = 0.05$$

$$L/D_p = 1.5$$

4 August 1994, T&I-212 O:\BGF\161119\94-3243.REP

The grout was prepared with a hand mixer. The mixing went on for approximately 5 minutes after the complete amounts of water and cement had been added.

The grout contact surfaces were wire brushed by hand tools between each test.

During the injection the grout was introduced from the bottom of the annulus and displaced air.

The grout used was a neat cement water paste using oil well G cement and a water/cement ratio of 0.3. The specification of the cement is given in Appendix A.

For each specimen a minimum of 6 cubes (100 mm) were casted from the same grout slurry as was injected.

Curing:

When only fatigue testing was to be performed the end faces of the grouted annulus were sealed and specimens were left to cure in a standard laboratory atmosphere (21^{0}C +/- 2^{0}C) for about 2 weeks until the desired grout strength was reached. In the case that early age cycling was performed the specimen was subjected to the specified displacement amplitude during grouting and curing. The displacement was applied with an electronically controlled hydrodynamic actuator. The actuator was set with a force limit such that when the maximum force was reached the sinusoidal displacement cycling was continued in force control. It was observed that the relative displacement between the pile and the sleeve ceased almost immediately after transfer to force control. As a consequence cycling was terminated when the load limit was reached in the latter tests.

4.2 Early age cycling

The relative displacement between the pile and the sleeve during the installation offshore is according to our experience typically 4 mm. Since the dimensions of our test specimen is approximately one quarter of a full scale connection it is assumed that the corresponding relative displacement of the test specimen is 1 mm. The magnitude of the load amplitude is calculated based on the ratio of the drag term of the Morrison's equation for a summer wave to a 100 - years wave. The drag term is integrated up to the mean water level and a wave steepness of 1/7 and a water depth of 100.0 m are assumed for the calculations. This is a conservative assumption which leads to the expression given below for the early age cycling load.

$$F_w = \frac{1}{2} PC_P D\omega^2 \eta_A^{2.2} \left| \frac{\left(\frac{sinh2kh}{4} + \frac{kh}{2}\right)}{ksinh^2 kh} \right|$$

$$\frac{FW_{100}}{FW_1} = \frac{C_{B100}}{C_{B1}} \frac{\eta_{A100}^{2.2}}{\eta_{A1}^{2.2}} \approx \left(\frac{\eta_{A100}}{\eta_{A1}}\right)^{2.2}$$

$$F = \pm 0.25 \; F_{bu} \; (4/25)^{2.2} = 0.044F_{bu}$$

The equation used is the same one as used in Phase I for the calibration which again is the same as used by Moses for the calibration of API RP2A LRFD. The purpose of this estimate is to arrive at representative magnitude of the early age cycling load and is not a precise value for any specific location.

The early age cycling was performed using a Schenk hydrodynamic actuator with a rated capacity of 63 kN. The following settings were used:

Cycle type	:	Sinusoidal
Frequency	:	0.1 Hz
Stroke amplitude	:	1 or 0.3 mm (maximum)
Force amplitude	:	15 kN (maximum)

The actuator automatically switched into force control when the maximum force was reached.

4.3 Fatigue Testing

Fatigue testing was performed in the same way for all specimens, both those exposed to early age cycling and those not exposed. All specimens were exposed to the same load ratio R of -1. R is defined as follows :

$$R = \pm \frac{\tau_{min}}{\tau_{max}}$$

R = - 1 means that the specimen is subjected to equal amounts of tensile and compressive loading. The fatigue load was introduced with a Schenk hydrodynamic actuator with a rated capacity of 7500 kN. The following settings were used:

Cycle type	:	Sinusoidal
Frequency	:	0.2 to 1hz
Force amplitude	:	to suit grout strength
Stroke amplitude	:	Safety setting only

A limit was set on the stroke amplitude such that testing automatically halted if the stroke increased by more that about 50%.

4.4 Summary of specimens

The ten specimens tested consist of specimens subjected to the following loading:

- plain fatigue only
- monotonically increasing static load only
- early age cycling only
- early age cycling followed by fatigue testing

The details of the specimens are summarized in the table on the next page. The fatigue load amplitude is given as a percentage of the mean static load capacity according to the DnV equation.

On the following page 24, a table summarizing in the tests performed in Britain is provided. Eight of these test results have been received in a data exchange and these results are included in the presentation in Section 5.

Table 4.4.1 Test program

Test no.	Description	$S/\sqrt{R_p \cdot t_p}$	H	H/S	Load	f_{cu}
1	plain fatigue	6	10 mm	0.05	30%	60.0
2	plain fatigue	1	3 mm	0.08	30%	49.3
3	static	1	3 mm	0.08	-	59.6
4	fatigue test with early age cycling	1	3 mm	0.08	20% , 1mm	59.8
5	plain fatigue	1	3 mm	0.08	25%	67.5/82
6	early age cycling, split test	1	3 mm	0.08	1 mm	-
7	fatigue test with early age cycling	1	2 mm	0.05	20% , 0.3 mm	54.0
8	fatigue test with early age cycling	3	5 mm	0.05	30%	52.8/82
9	fatigue test with early age cycling	3	5 mm	0.05	30%	59.5
10	early age cycling, split test	3	5 mm	0.05	1 mm	-

D_p = 320 mm, t_p = 8 mm, D_s = 395 mm, t_s = 8 mm

Table 4.4.2

Fatigue tests performed in the U.K

No. of tests	Description	H/S	H
2	fatigue test with early age cycling	0.073	1.5 mm
8	fatigue test with early age cycling	0.06	1.3 mm
5	plain fatigue	0.06	1.3 mm
1	static test with early age cycling	0.06	1.3 mm
1	static test with early age cycling	0.012	
1	fatigue test with early age cycling	0.012	
2	fatigue test with early age cycling	0.036	1.5 mm
1	fatigue test with early age cycling	0.06	1.3 mm
3	fatigue test with early age cycling	0.036	1.5 mm

D_p = 324 mm, t_p = 9.5 mm, D_s = 355 mm, t_s = 4.3 mm

5 TEST EXECUTION

5.1 Specimen no 1

Test specimen no 1 was subjected to plain sinusoidal fatigue testing.

Load amplitude	:	1000 kN (30% Pu)
amplitude	:	1.25
Endurance	:	10 cycles

Fig. 5.1.1 shows a load displacement record of the first cycles

5.2 Specimen no 2

Test specimen no 2 was subjected to plain sinusoidal fatigue testing.

Load amplitude	:	1800 kN (30% Pu)
Length to diameter ratio	:	1.50
Endurance	:	1300 cycles

The testing was initially started with a stress amplitude of 800 kN. The recorded load displacement curve is shown in Fig. 5.2.1. The specimen was run for 10000 cycles at this load level. Fig. 5.2.2 shows the load displacement curve at 650 cycles. As there was no evidence of degradation in the form of increasing displacements the load amplitude was increased to 1200 kN. In the front cycle the displacement was 0.17 mm. It increased to 0.32 mm in a few cycles and then stabilized. As soon as the load was increased the displacement increased further increased to 0.59 mm. The displacement continued to increase gradually for the first 1000 cycles. There after displacements began to increase significantly faster. Failure was recorded at 1300 cycles. Fig. 5.2.3 shows a load displacement plot recorded immediately before failure.

5.3 Specimen no 3

This test was a plain static test and was performed to obtain an improved reference value for the static strength of specimens with this configuration.

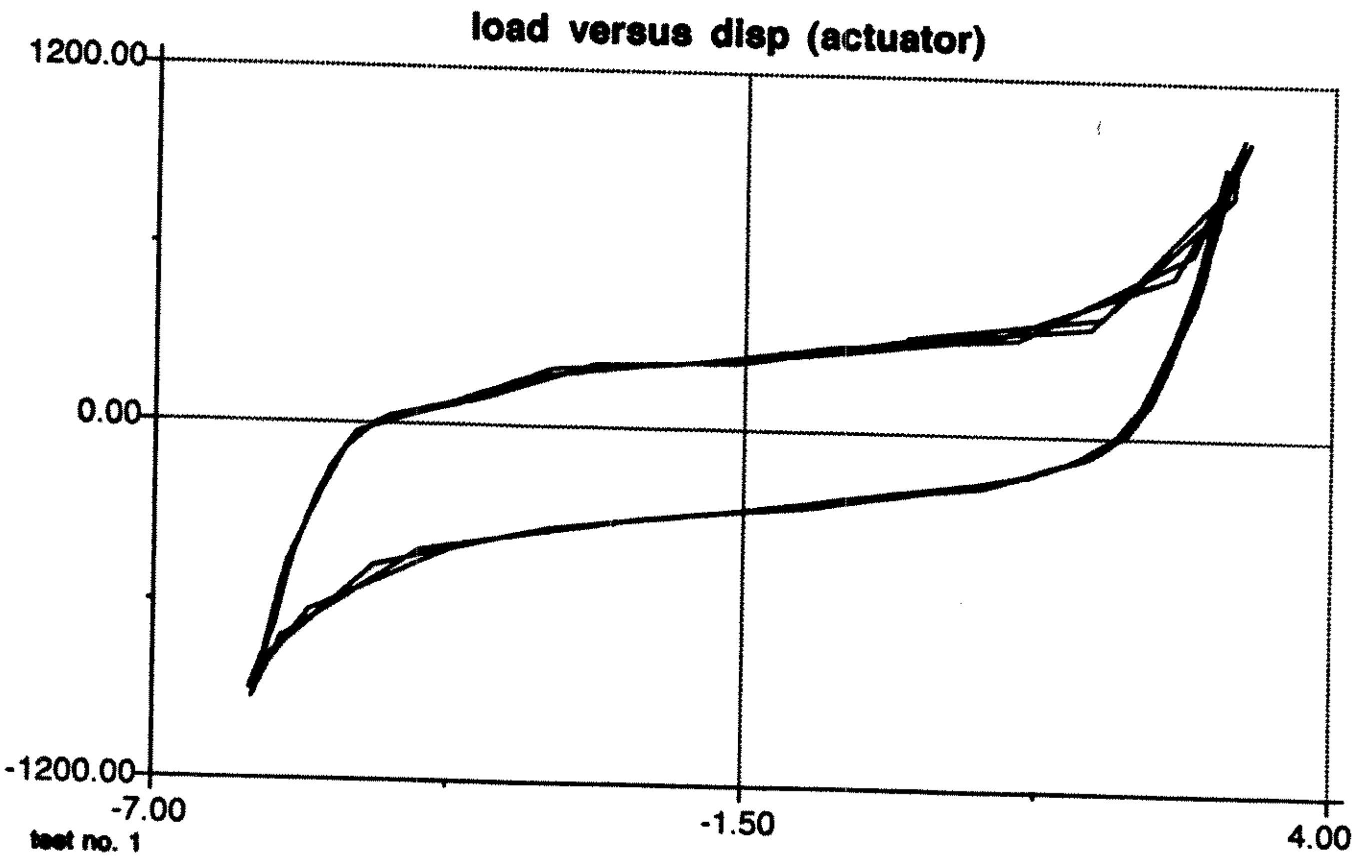

Figure 5.1.1 Test no. 1 Load displacement record

Grouted pile sleeve test no. 2

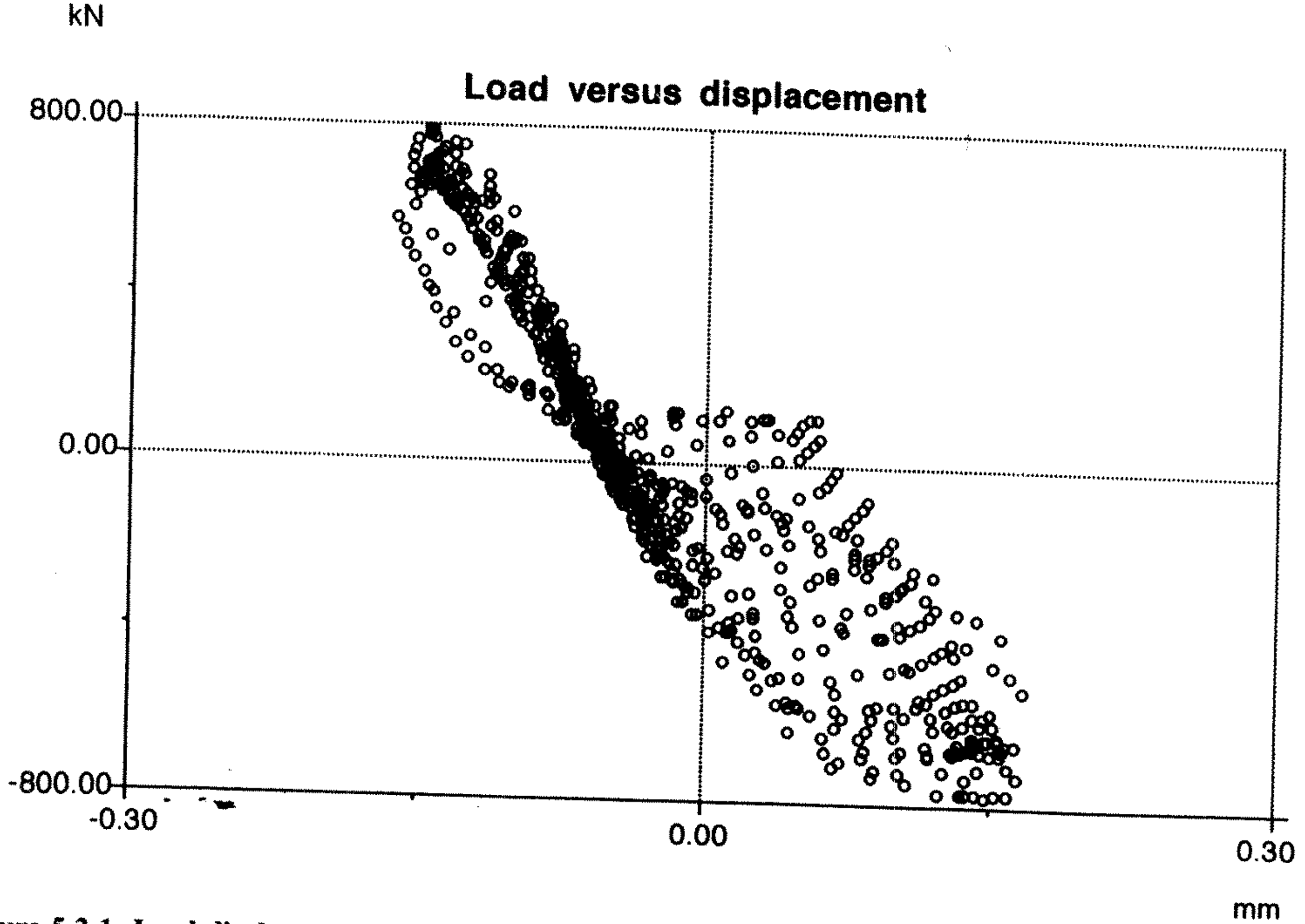

Figure 5.2.1 Load displacement record at test commencement

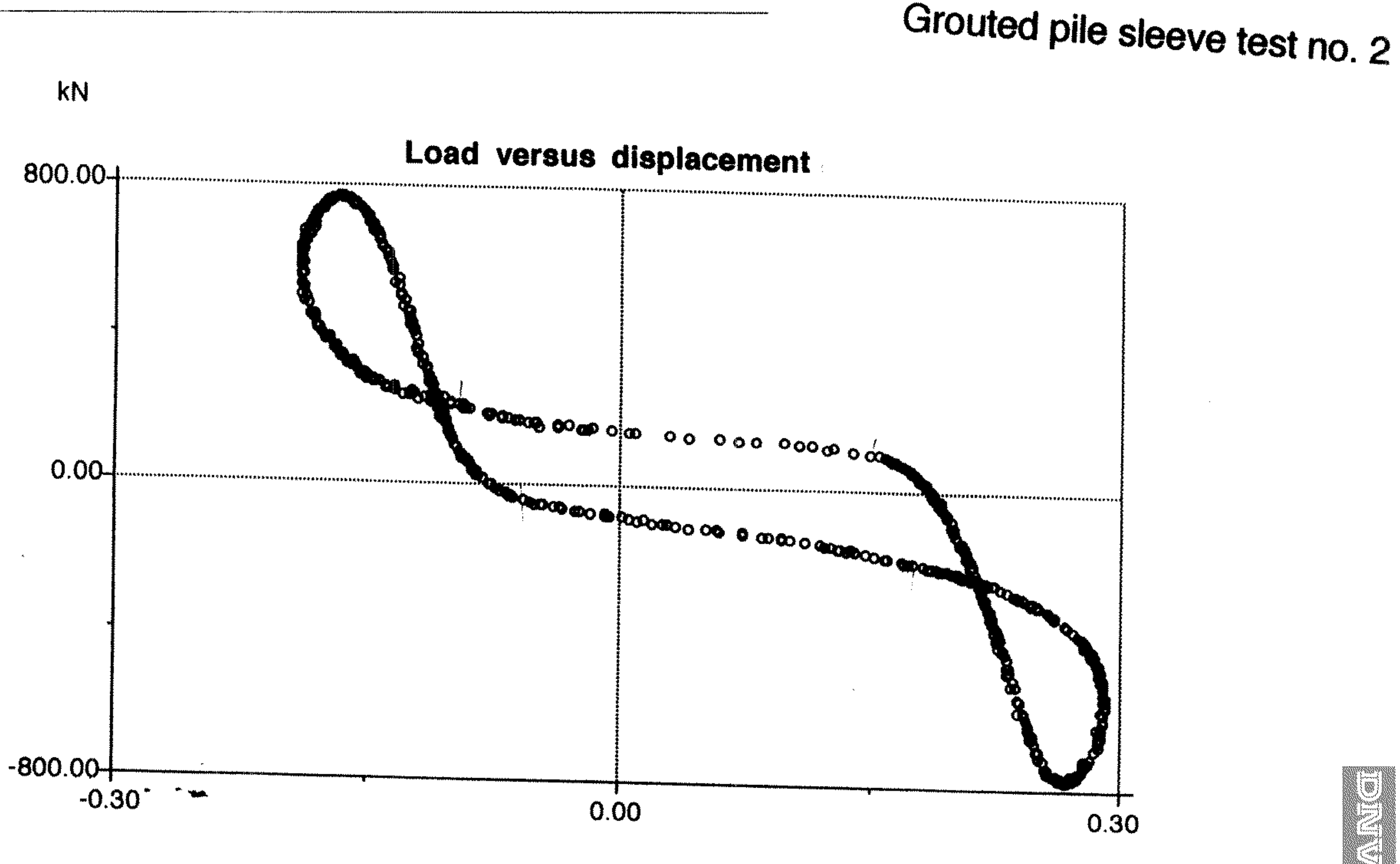

Figure 5.2.2 Load displacement record at 650 cycles

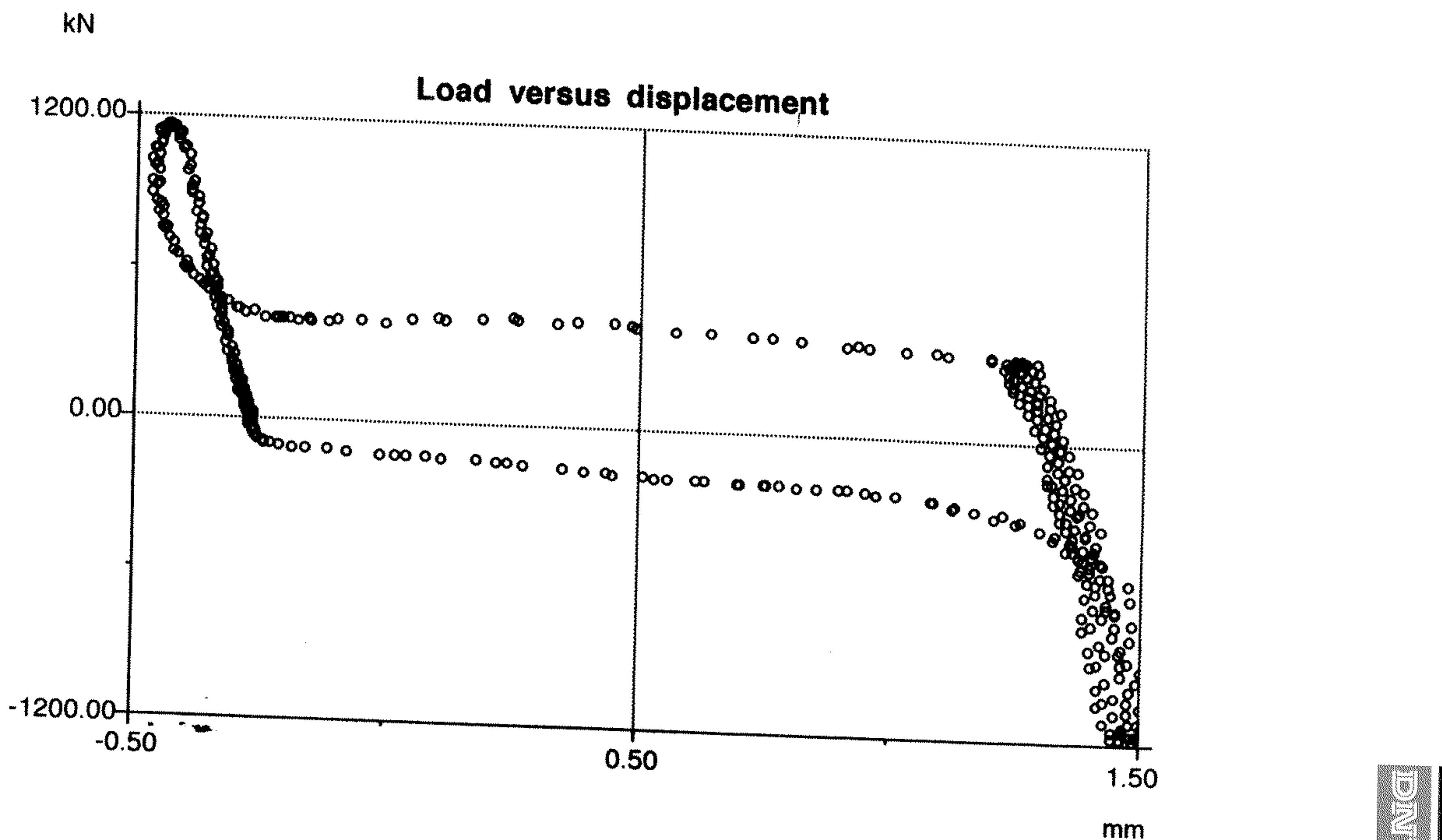

Figure 5.2.3 Load displacement record immediately before failure

Grouted Pile Sleeve test no. 3

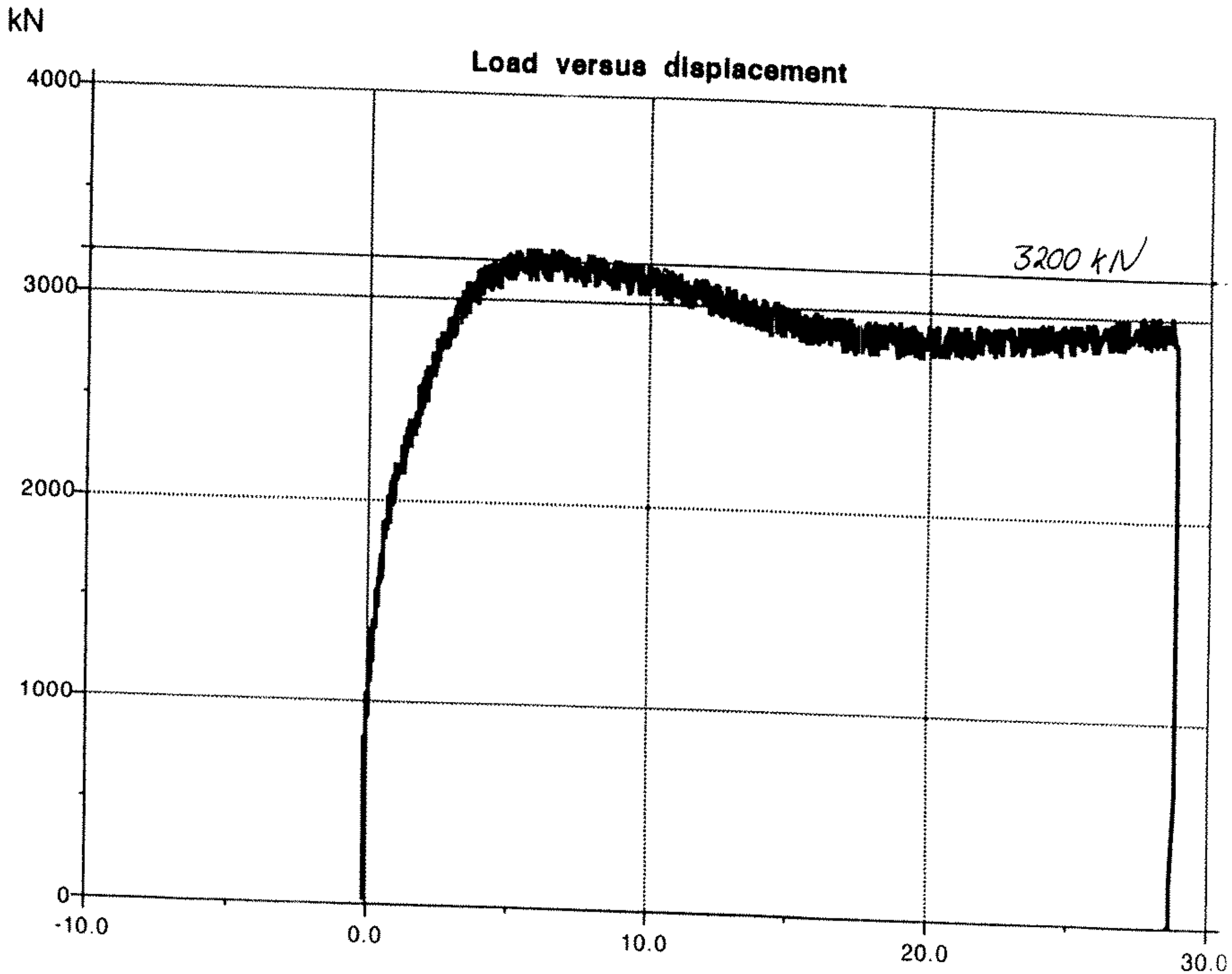

Figure 5.3.1 Grouted pile sleeve test no. 3

Length to diameter ratio	:	1.50
Recorded ultimate strength	:	3200 kN

The load deformation plot is shown in fig. 5.3.1.

5.4 Specimen no 4

Test specimen no 4 was first subjected to plain sinusoidal early age cycling and then to plain sinusoidal fatigue testing.

Early age cycling displacement amplitude	:	1.0 mm
Fatigue load amplitude	:	600 kN
Length to diameter ration	:	1.50
Endurance	:	100 cycles

Figure 5.4.1 shows Load displacement records obtained in the course of the test. At failure it was observed that the grout fragments had a configuration indicating that the failure had been through the grout matrix in a plane tangential to the top of the shear keys.

5.5 Specimen no 5

Test specimen no 5 was subjected to plain sinusoidal fatigue loading only:

Fatigue Load amplitude	:	900/1100 kN
Length to diameter ration	:	1.50
Endurance	:	1220 + 47 630 cycles

Due to failure of the end fixtures this test was run in two parts. In the second part of the test the load amplitude was increased to reflect the increase in cube strength. The load amplitude was thus maintained at 25% of the ultimate strength throughout the test.

5.6 Specimen no 6

In order to verify the observations of the failure mode of specimen no 4 one specimen with only early age cycling was run.

Displacement amplitude	:	1.0 mm
Length to diameter ration	:	1.50

Grouted pile sleeve test no. 4

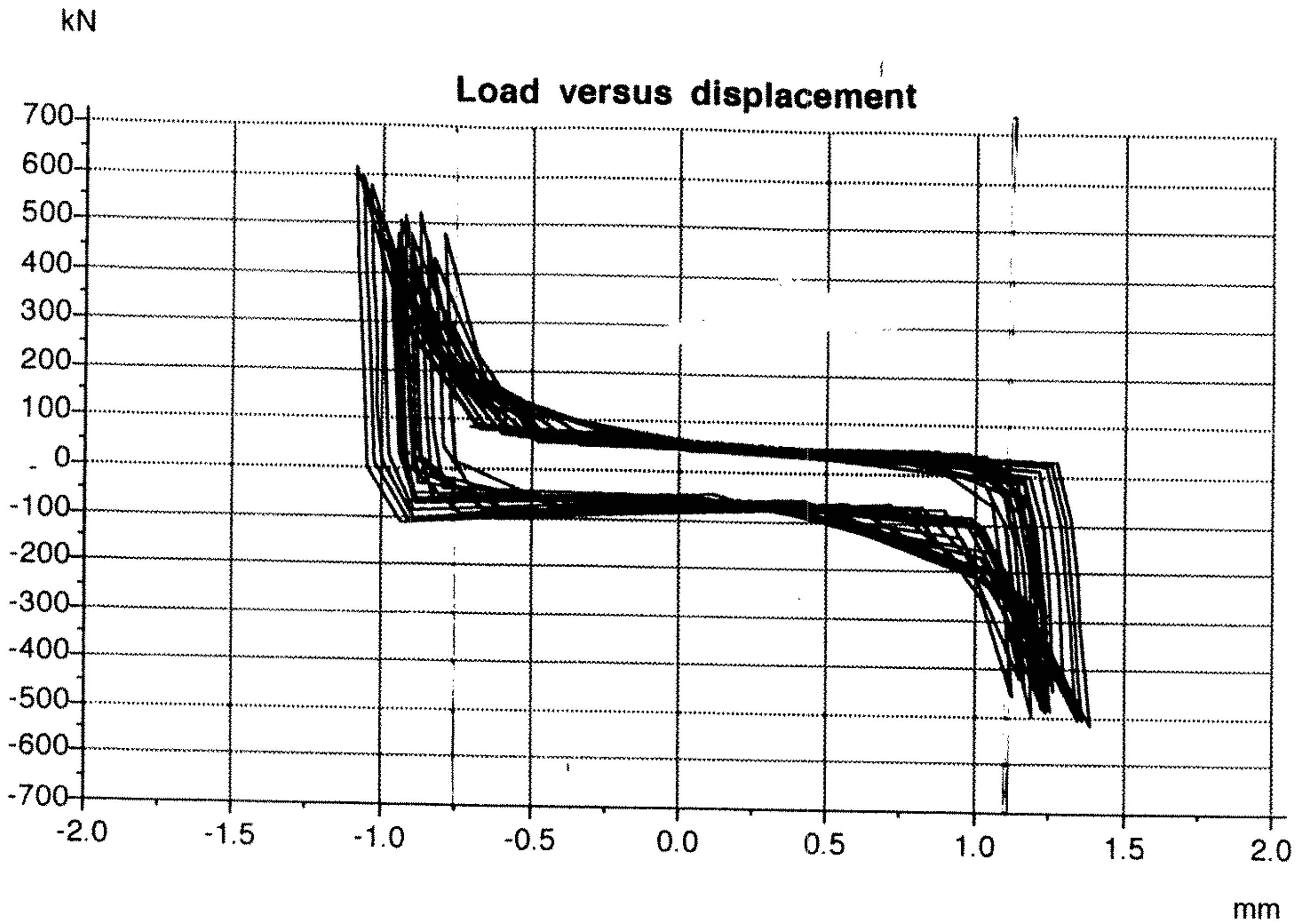

Figure 5.4.1 Grouted pile sleeve test no. 4

After cycling the specimen was sectioned longitudinally. A very narrow band of darkened grout was observed in the plane tangential to the top of the shear keys on the pile. This is shown diagrammatically in Fig. 5.6.1. It is evident that the specimen has suffered partial segregation or bleeding in this zone and has a greatly increased water-cement ratio which in turn leads to substantial loss of strength.

The following report was obtained from laboratory investigation using optical microscopy, scanning electron microscopy and energy dispersive x-ray spectroscopy.

MICROSCOPIC EXAMINATION OF NORWELL CLASS G OIL WELL CEMENT GROUT SPECIMEN:

Oil Well cement grout has been cast between two steel pipes. During testing of the specimen had been subjected to cycling load during curing.

Longitudinal sectioning of the pipes obtained after testing revealed two lines in the cement close to the inner surface of the pipe parallel to the test load direction. Whether these lines were cracks or not was to be determined. A possible difference in chemistry in the lines compared to the adjacent material should also be established.

Two samples were prepared for examination. A specimen with a fractured surface and a specimen with a ground surface were subject to examination. Grinding of the specimen revealed a darker grey layer towards the surface of the inner pipe in which the two observed lines were located. Figure 5.6.2 shows the layer and the here denoted base material. The specimens were prepared with a thin gold layer on the surface prior to examination in a scanning electron microscope (SEM). Attached to the microscope is an energy dispersive X-ray spectrometer (EDS) which was applied for microanalysis of the specimens. The system detects elements down to and including flouring in the periodic system. Consequently oxygen, nitrogen and so on cannot be detected.

SEM/EDS Examination

Figure 5.6.3 shows a photo of the two lines as they appear on the fractured specimen. The lines appear darker than the adjacent material. The contrast is caused by a difference in chemistry between the material in the lines and the adjacent material. The applied scanning mode distinguishes between lighter elements as darker components compared to heavier elements.

The appearance of the lines is darker which should indicate a difference in chemistry. EDS analysis was carried out in the lines, in the adjacent material and in the "base" material. See Fig. 5.6.9, 5.6.10 and 5.6.11. The analysis revealed the elements calcium (Ca), silicon (Si) and minor amounts of magnesium (Mg), aluminium (Al) and iron (Fe). The analysis showed no distinct difference in chemistry in the various areas. Consequently, the difference in chemistry detected in figure 2 is most probably caused by elements lighter than fluorine, which can not be identified by the equipment.

A study of the lines at higher magnification revealed a porous structure within the lines, see figure 5.6.4, 5.6.5 and 5.6.6. A crack in the line close to the inner surface of the pipe was revealed.

An examination of the fracture appearance carried out both in the lines, in the dark grey surface layer and in the base material, showed some variation in the structure (figure 5.6.7 and 5.6.8).

The appearance in the dark grey surface layer deviates most from the structure seen in the lines and in the "base" material. It seems that the examined areas represent different levels in the reaction process.

EARLY AGE CYCLING - SPLIT TEST

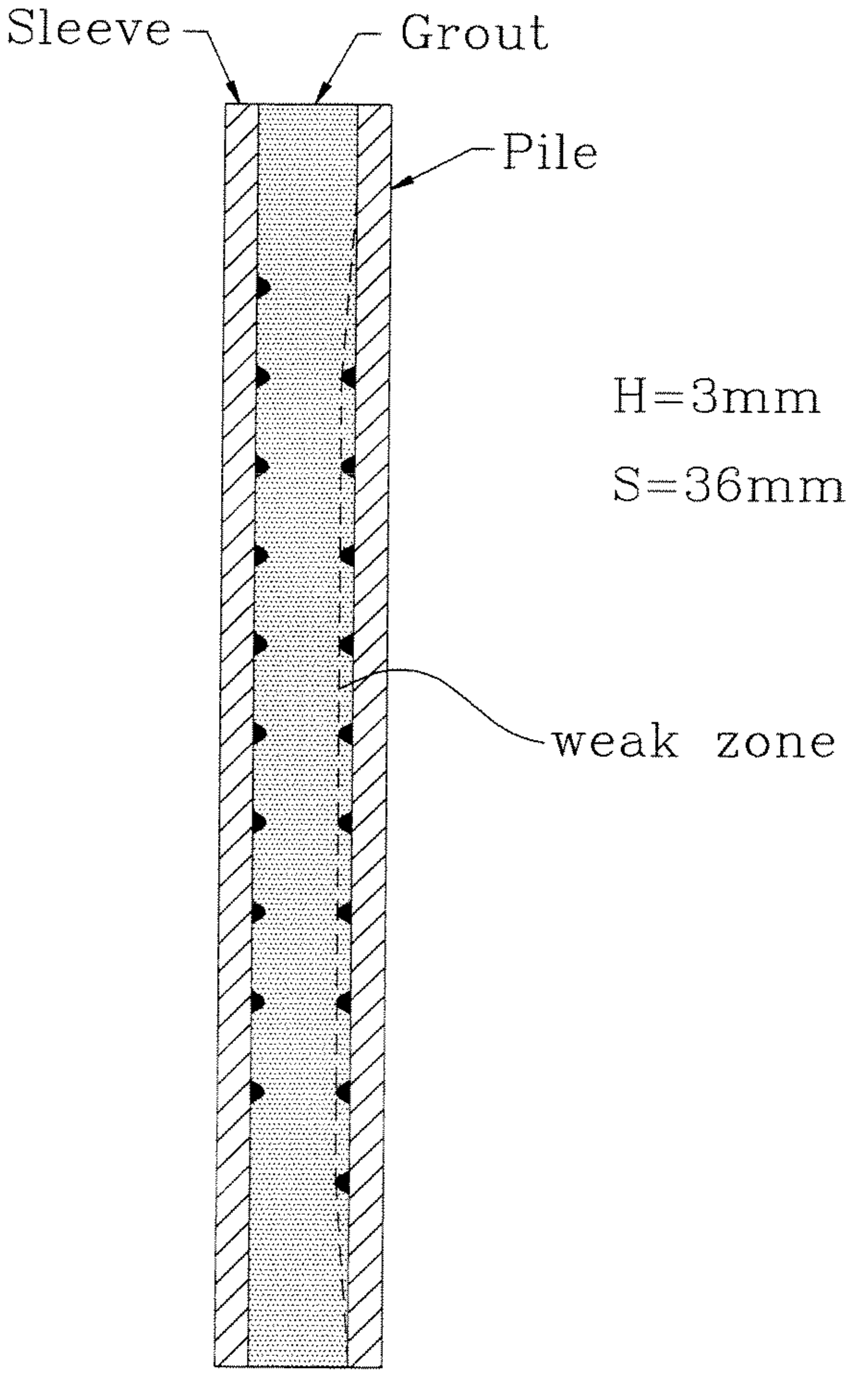

Figure 5.6.1 Location of band of disturbed grout

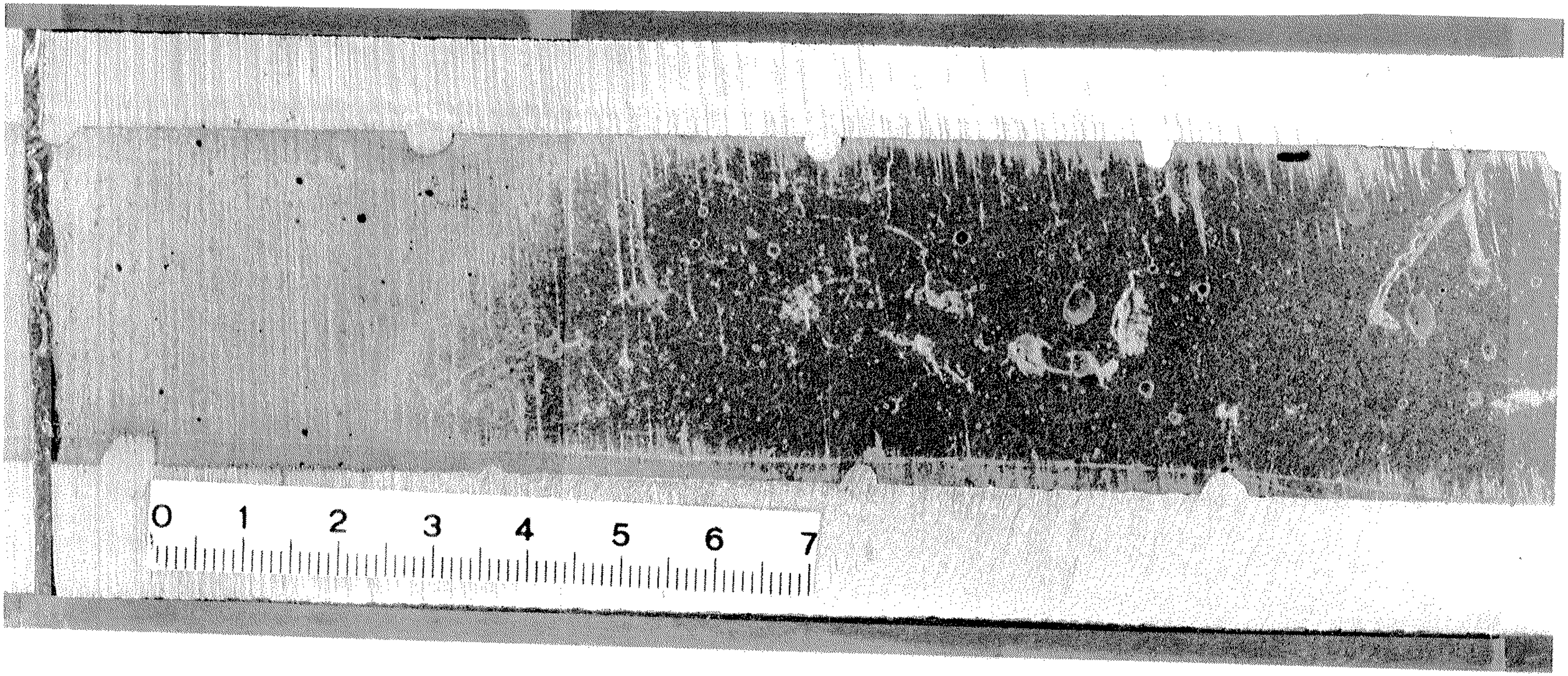

Figure 5.6.1 Location of band of disturbed grout

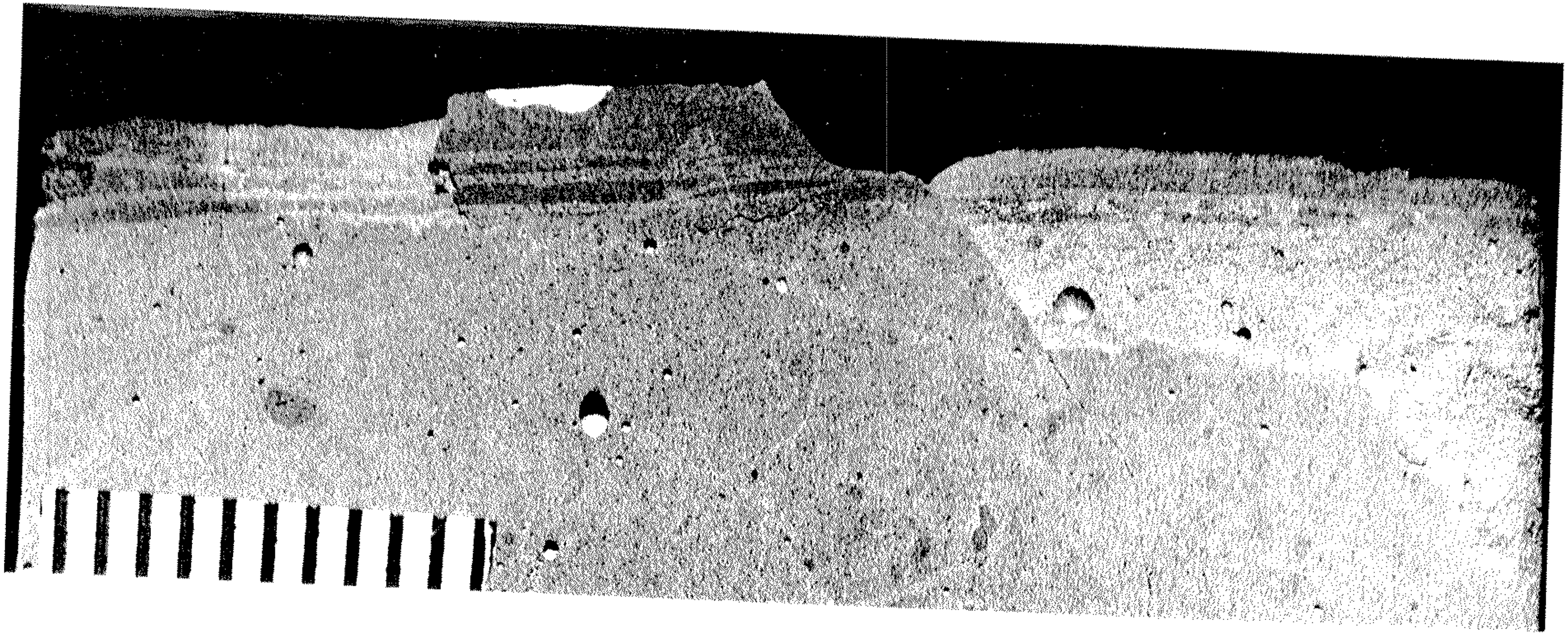

Fig. 5.6.2 The ground specimen with the dark grey layer towards the top of the photo is revealed. Magnification 6X.

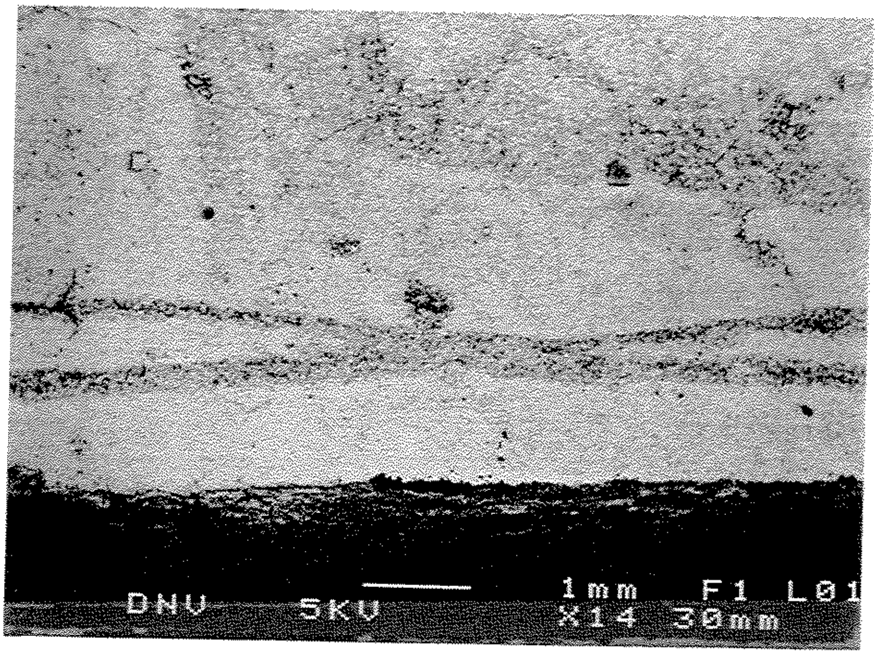

Fig. 5.6.3 The two lines towards the surface of the inner pipe as they appeared in the fractured specimen. Magnification 14X

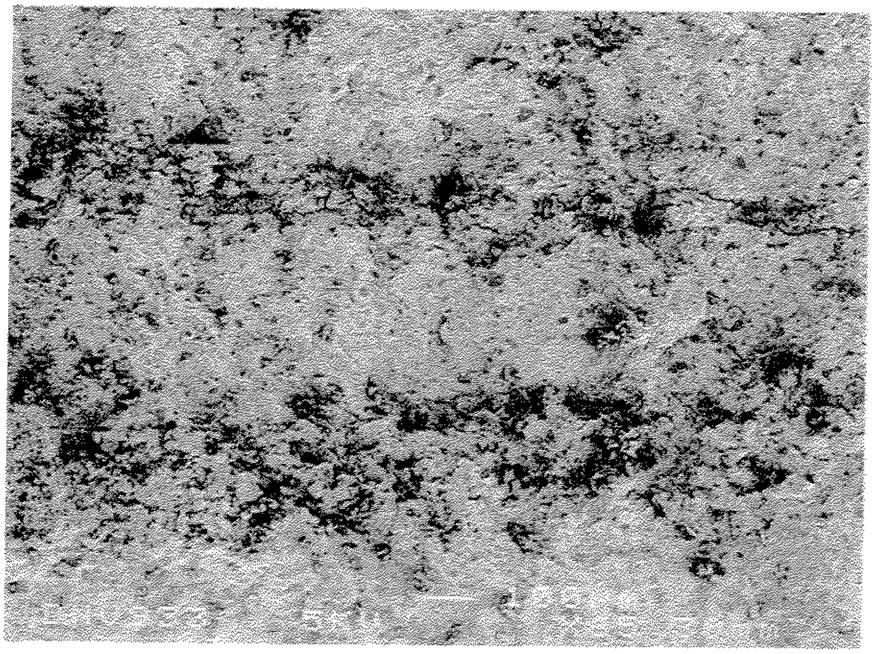

Fig. 5.6.4 The parallel lines are shown. The surface of the inner pipe is positioned towards the bottom of the figure. A crack - like pattern is observed in the bottom line. Magnification 40X

Fig. 5.6.5 The parallel lines in another area of the specimen. The same crack - like pattern as in figure 3. is observed in this figure. Magnification 65X.

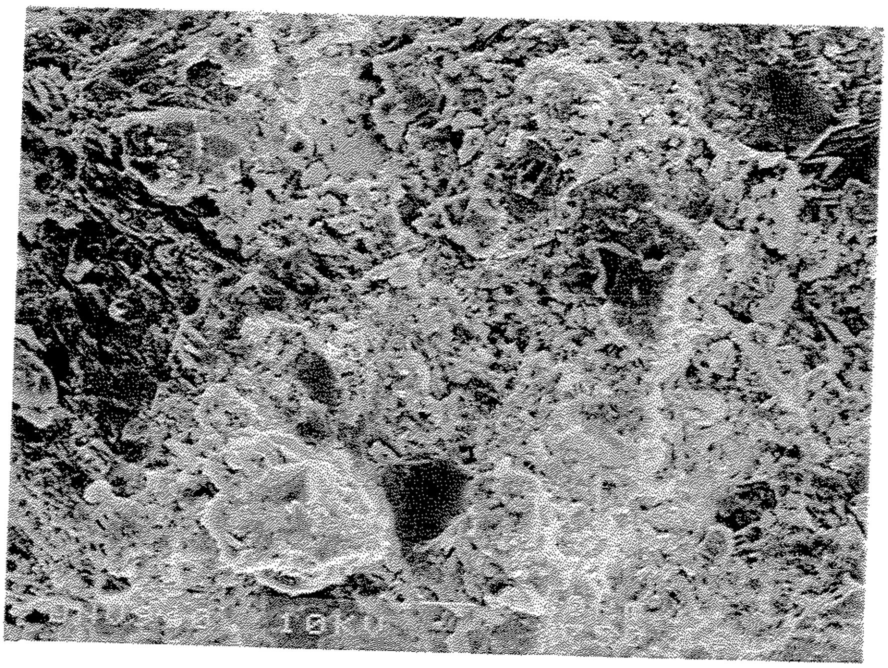

Fig. 5.6.6 The fracture appearance in the dark grey surface layer is shown. Magnification 750X.

Fig. 5.6.8 The fracture appearance in the "base material". Magnification 750X.

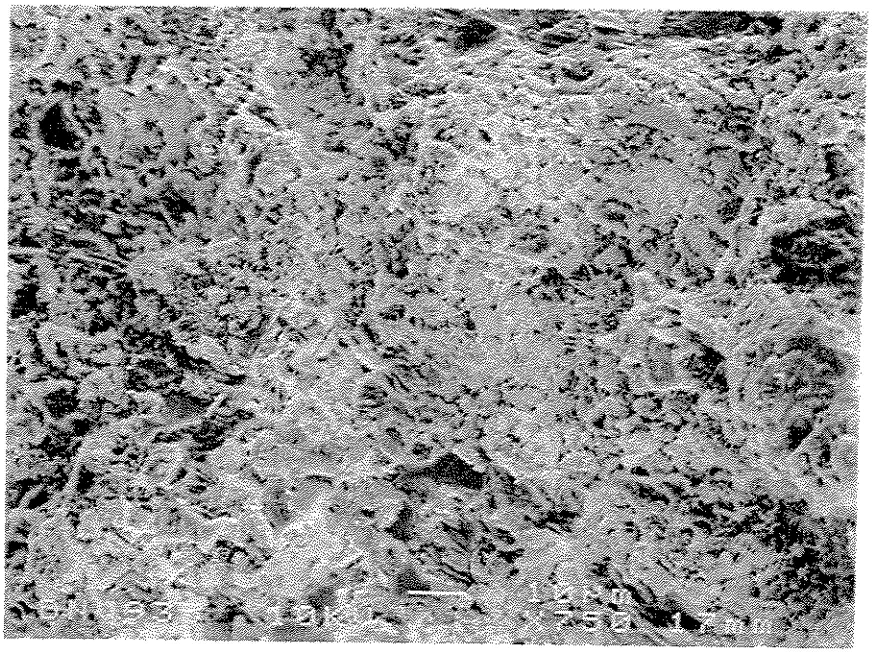

Fig. 5.6.7 The fracture appearance in the lines observed in the figures above. Magnification 750X.

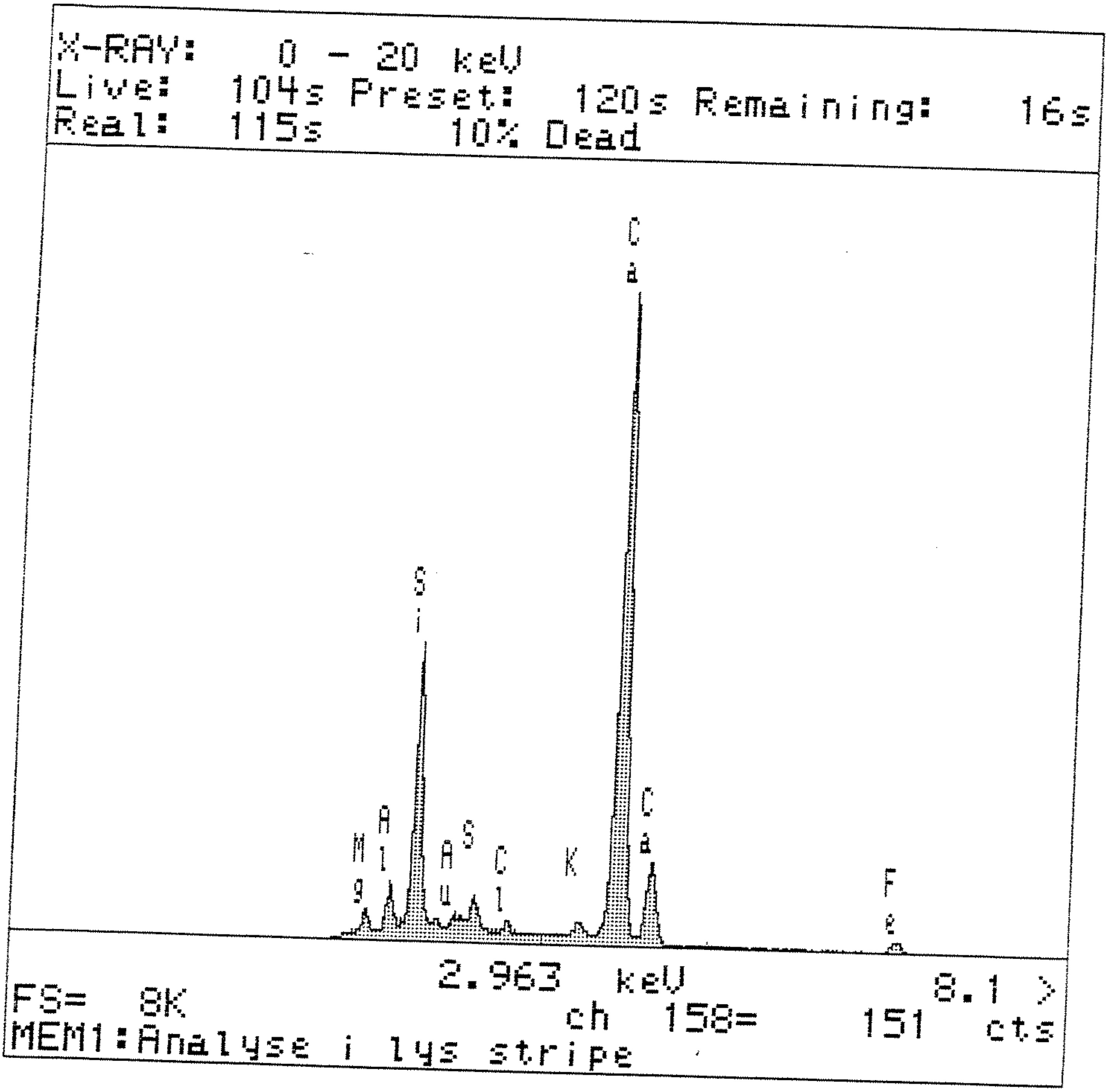

Figure 5.6.9 EDS of disturbed grout material

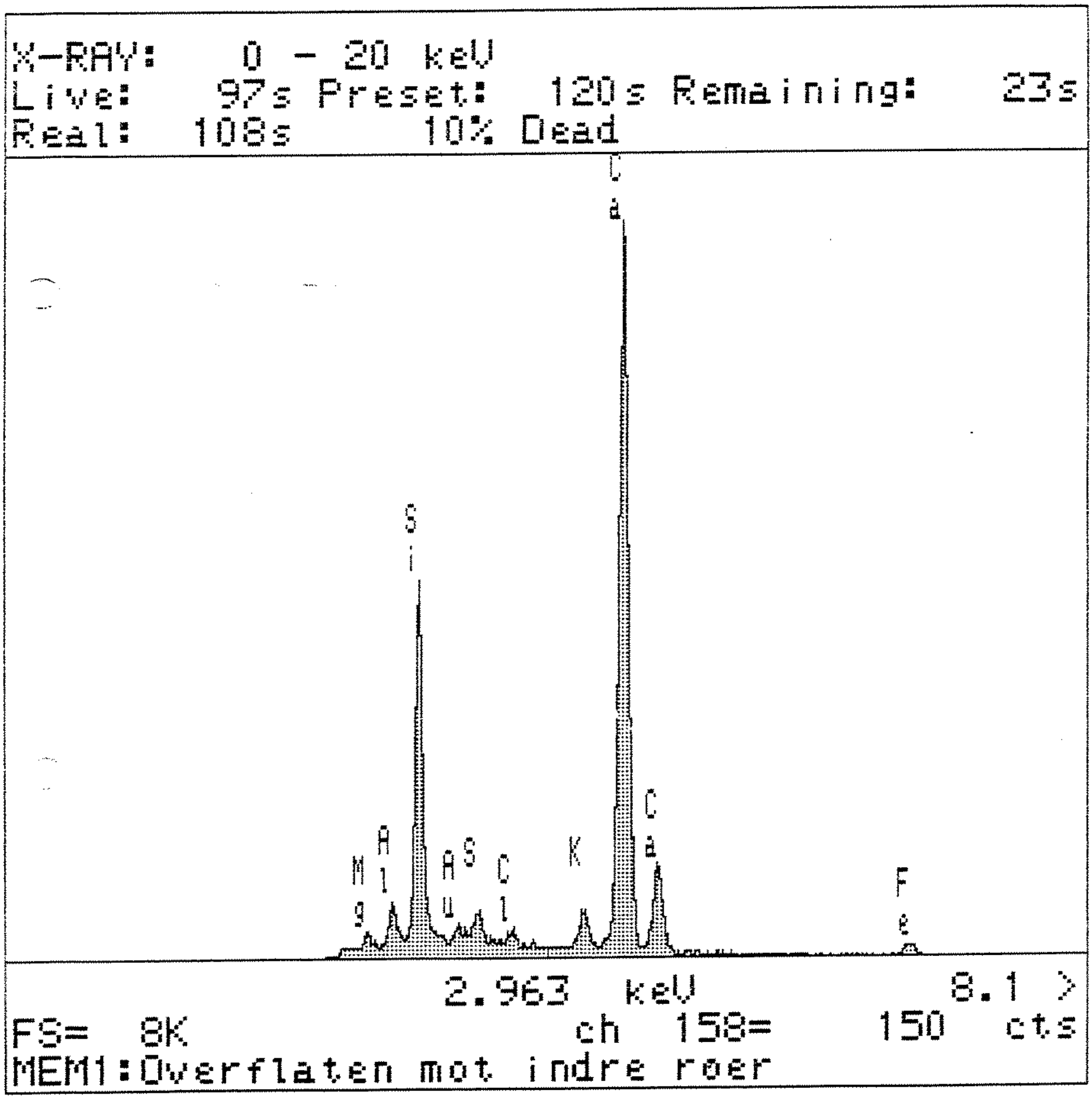

Figure 5.6.10 EDS of material close to steel interface

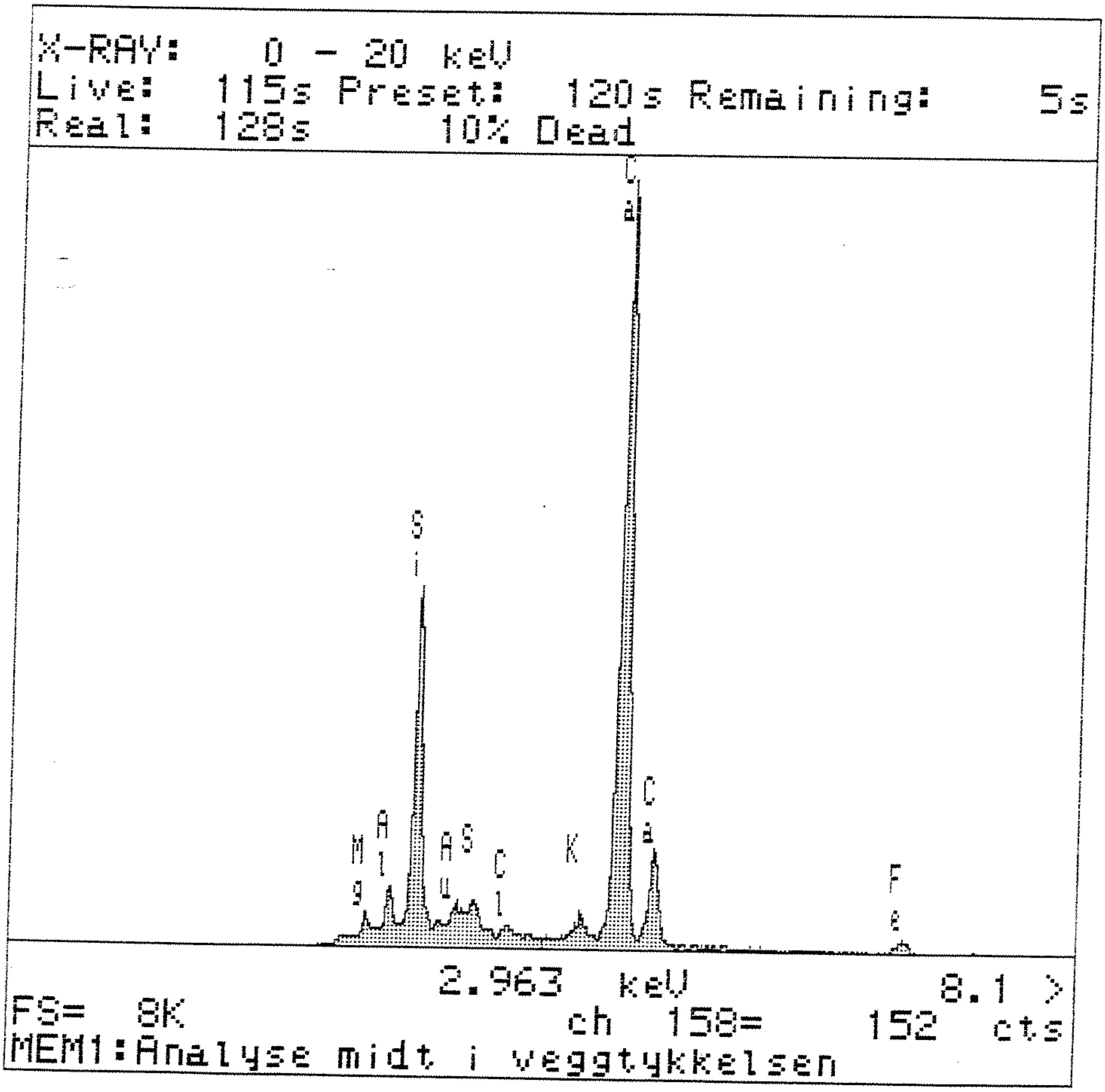

Figure 5.6.11 EDS of undisturbed grout

5.7 Specimen no 7

Test specimen no 7 was subjected to plain sinusoidal early age cycling with a reduced amplitude to determine the effect of this on fatigue. Then it was subjected to a fatigue test:

Early age cycling displacement amplitude	:	0.3 mm
Fatigue load amplitude	:	600 kN
Length to diameter ratio	:	1.50
Endurance	:	4540 cycles

The recorded displacement range is shown in figure 5.7.1 as a function of the number of cycles.

5.8 Specimen no 8

Test specimen no 8 was also subjected to plain sinusoidal early age cycling, followed by a plain sinusoidal fatigue test:

Early age cycling displacement amplitude	:	1.0 mm
Fatigue load amplitude	:	650/800 kN
Length to diameter ratio	:	1.50
Endurance	:	> 1 019 570 cycles

During the fatigue testing a failure of the actuator electronics occurred. When the test was restarted the load was increased to reflect the increased grout cube compressive strength. Throughout the test the displacement remained between 1.1 mm and 1.2 mm. The test was run to 1 million cycles and recorded as a run-out.

This test was initially started up at a low frequency of about 0.2 hz. The frequency was gradually increased to 1 hz when it was seen that this had no adverse effect on the specimen.

5.9 Specimen no 9

Test specimen no 9 was a repeat of test specimen no 8:

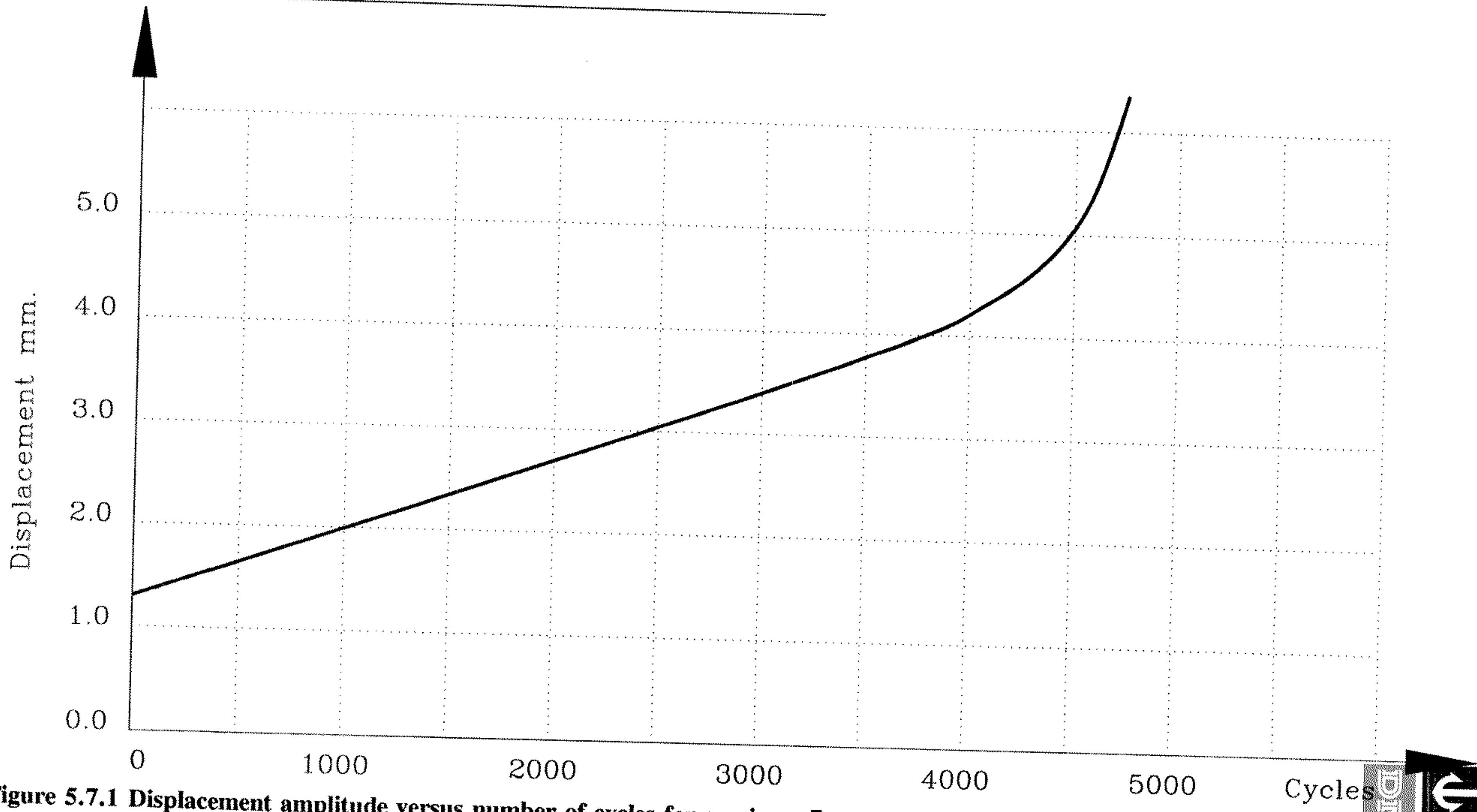

Figure 5.7.1 Displacement amplitude versus number of cycles for specimen 7

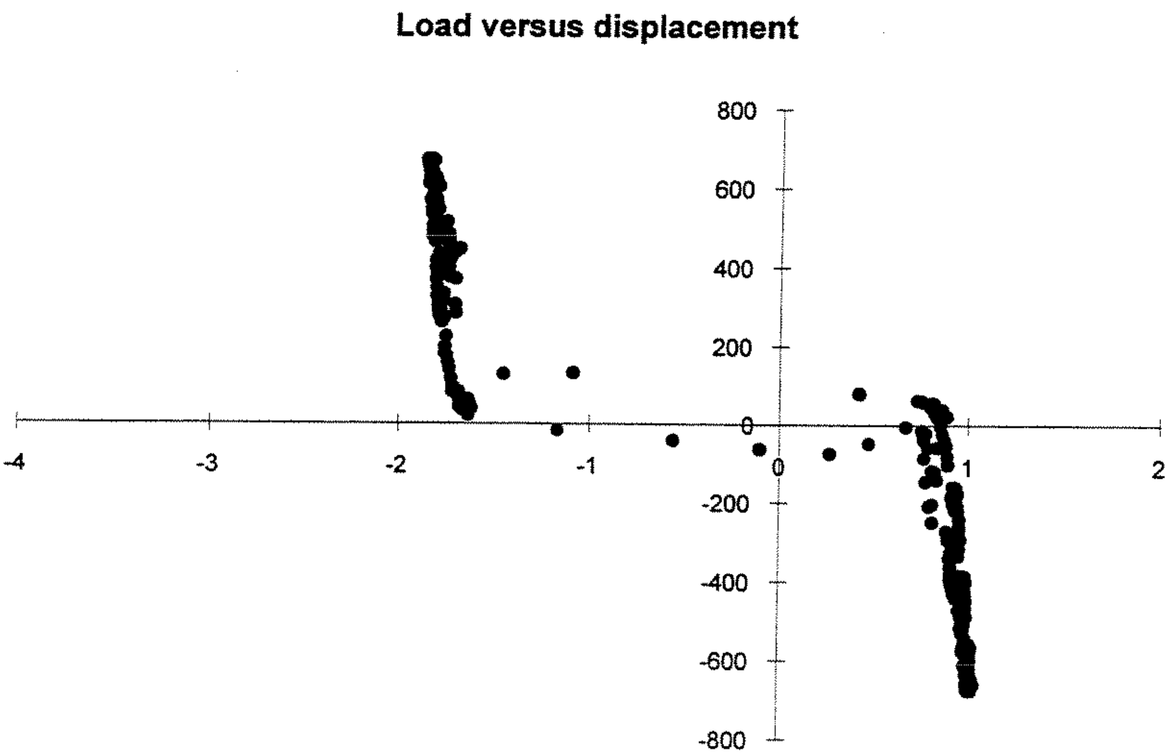

Figure 5.9.1 Recorded displacements at 1000 cycles

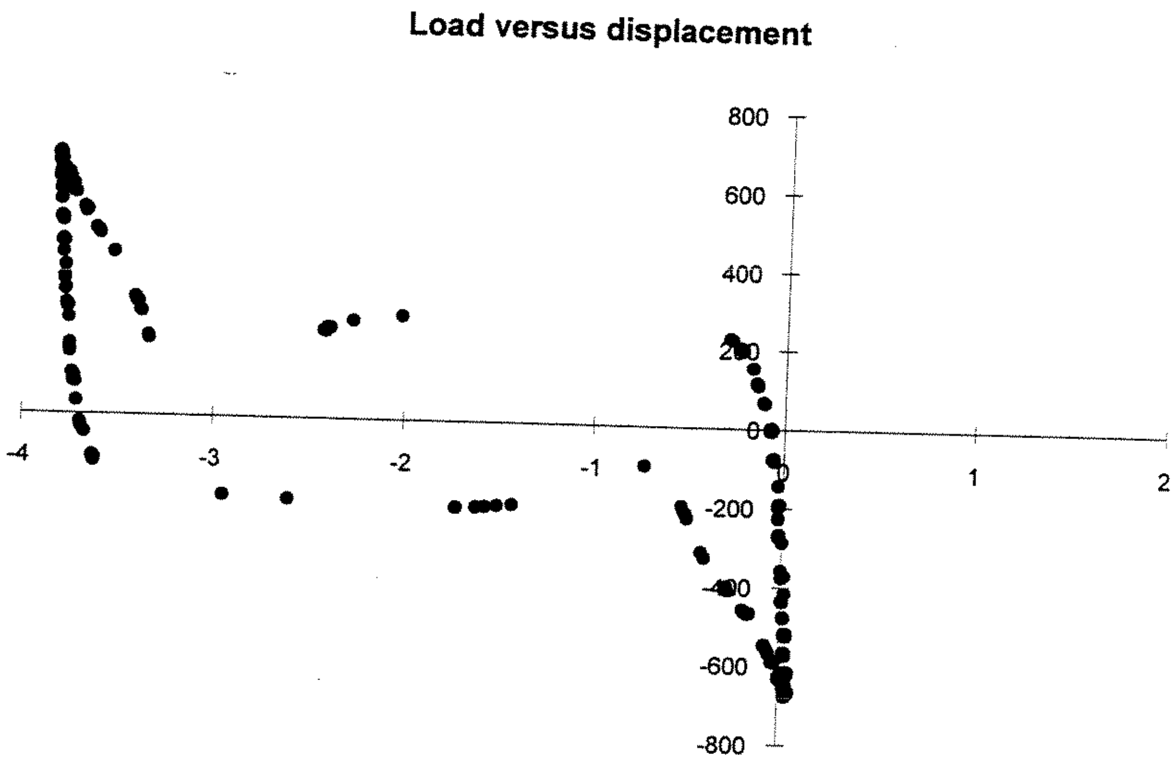

Figure 5.9.2 Recorded displacements at 25000 cycles

Early age cycling displacement amplitude	:	1.0 mm
Fatigue load amplitude	:	650 kN
Length to diameter ratio	:	1.50
Endurance	:	48410 cycles

Based on the experience from specimen no 8 this specimen was from the outset cycled at 1 hz. It was observed that the displacement increased from 1 mm at the outset to 4 mm very rapidly and the actuator which was running in force control appeared to exserting an adverse effect by impacting at the top and the bottom of the cycle. To deviate this the frequency was reduced to 0.3 hz and the oil supply was chocked.

After the above adjustment the displacement stabilized at about 4 mm from which it increased very slowly.

5.10 Specimen no 10

Specimen no 10 was subjected to early age cycling only and the sectioned longitudinally.

Early age cycling displacement amplitude	:	1.0 mm
Length to diameter ratio	:	1.50

It was clearly observable that there was a disturbed zone similar to that found in specimen no 6. (Due to a rougher method of sectioning the disturbed zone had cracked) The trajectory of the disturbed zone was observed to differ from that of specimen no 6 in that it between shear keys deflected out to the steel interface. This is shown in Figs. 5.10.1, 5.10.2 and 5.10.3.

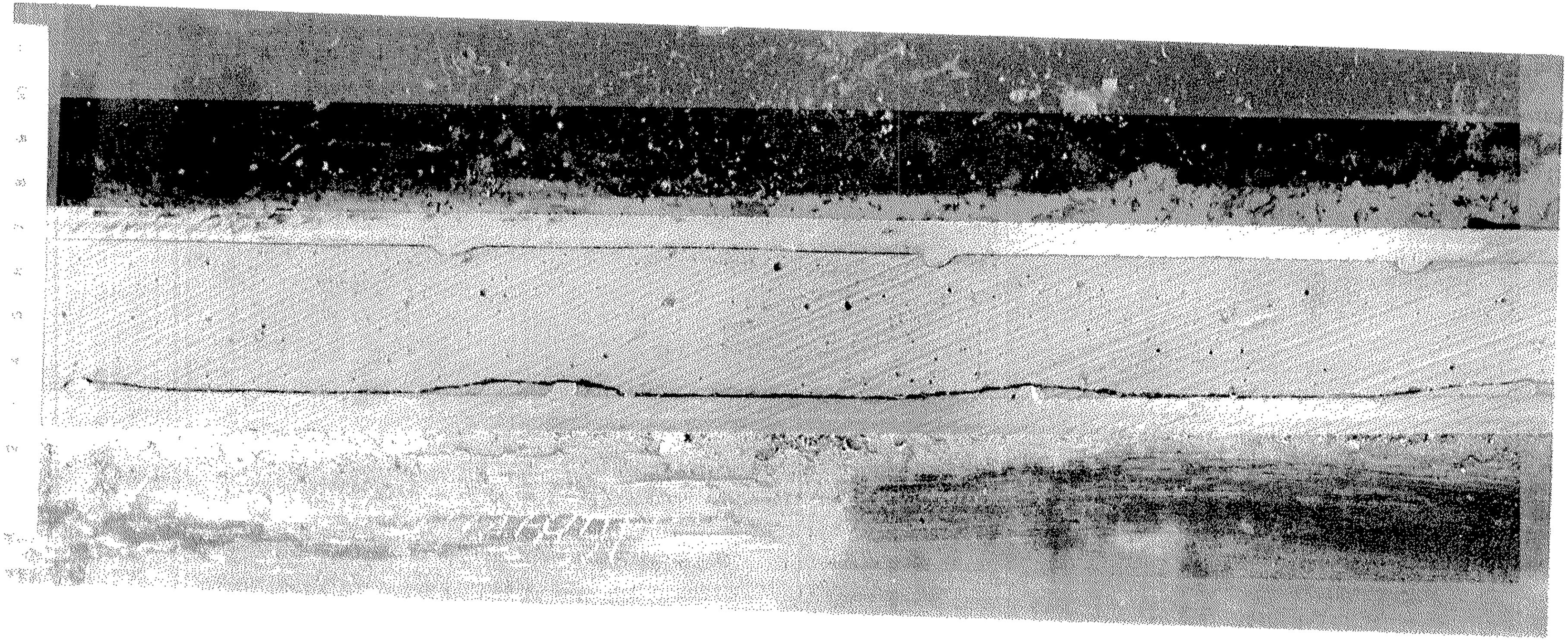

Figure 5.10.1 General view of trajectory of disturbed zone

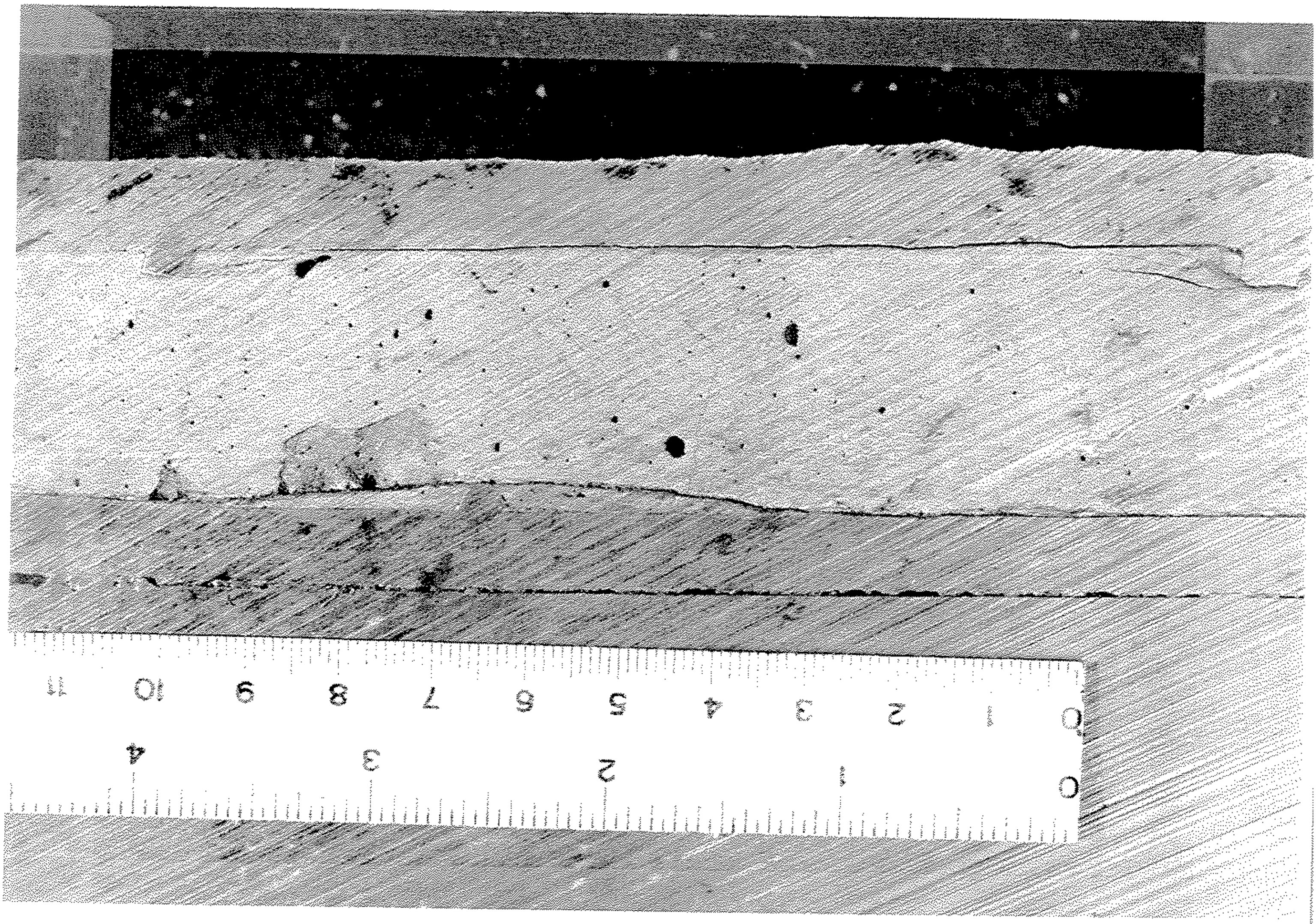

Figure 5.10.2 Close view of disturbed zone trajectory at a shear key location

Figure 5.10.3 Local detail of disturbed zone

5.11 Test results received from the UK project

A set of eight test results have been received in a data exchange with a project executed in the UK /10/. The specimens are numbered as follows:

Test no.	Cube strength at test
4 - 7	62.3 MPa
4 - 8	47.5 MPa
4 - 8A	49.4 MPa
4 - 8R	See data sheet
4 - 16	See data sheet
4 - 17	See data sheet
4 - 18	See data sheet
4 - 19	See data sheet

The test results are given in the following data sheets.

4 August 1994, T&I-212 O:\BGF\161119\94-3243.REP

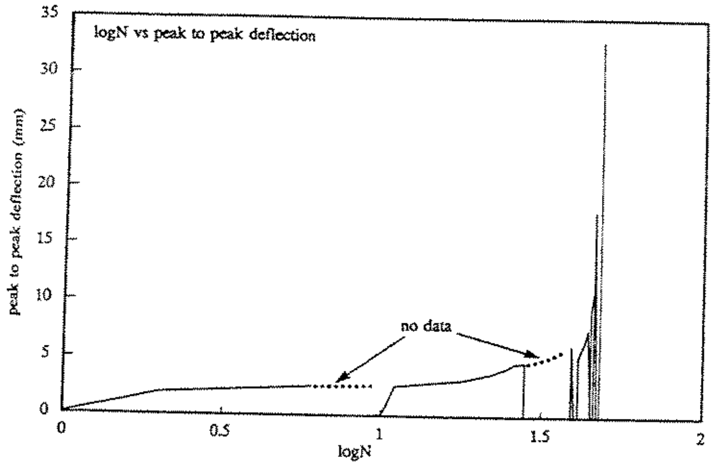

TEST NO 4 - 7

weld bead height to spacing ratio	h_{min}/s h_{av}/s	0.063 0.065
early age displacement	$\pm\ \delta/D$	0.0034
applied load / predicted static capacity	P/S	0.39
actual static capacity, post fatigue test	kN	1158
equivalent estimated static capacity (without fatigue test)	kN	2264
actual static capacity / equivalent predicted value		0.51
cycles to first 'failure'		48
final number of cycles achieved (R=runner)		48

During early age cycling, the pile remained static whilst the sleeve was moved.

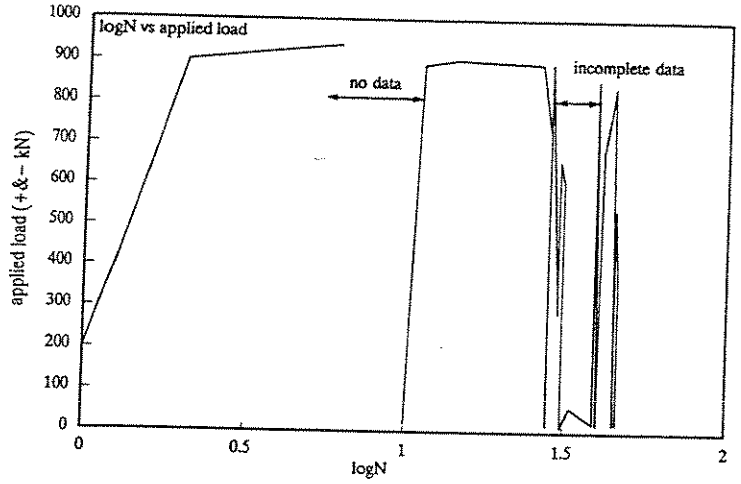

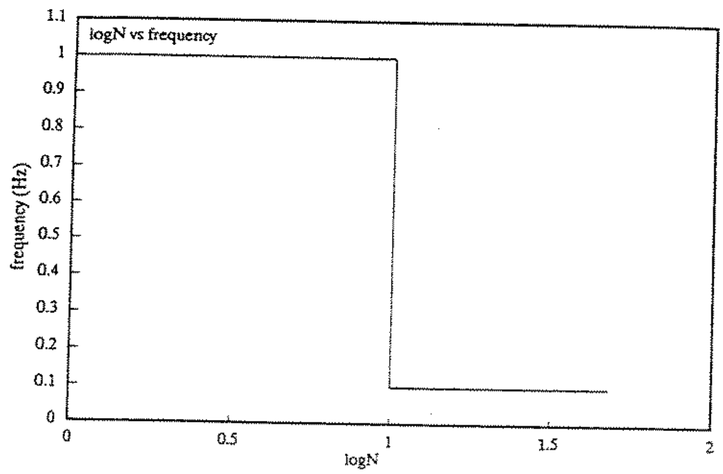

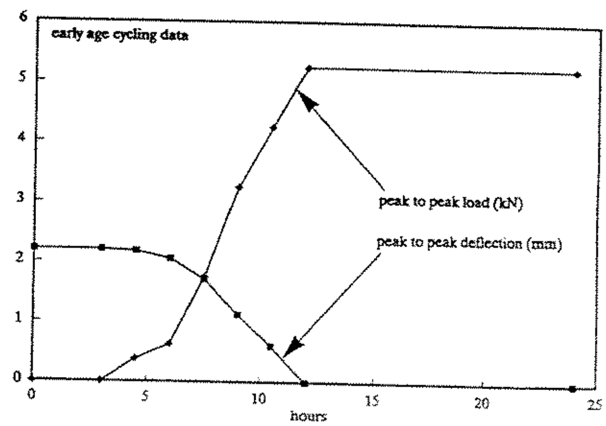

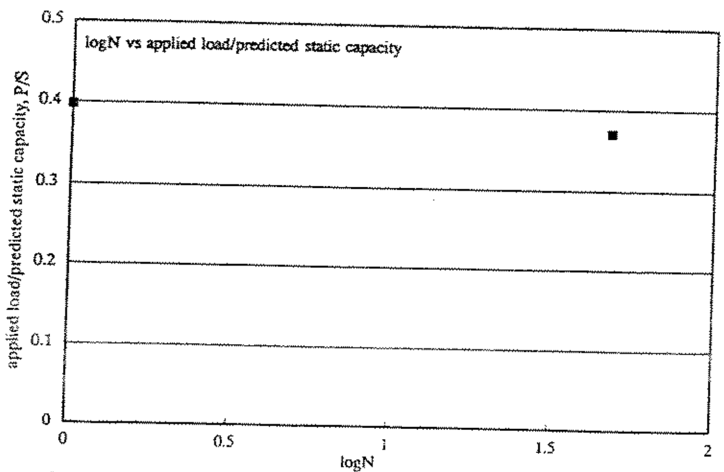

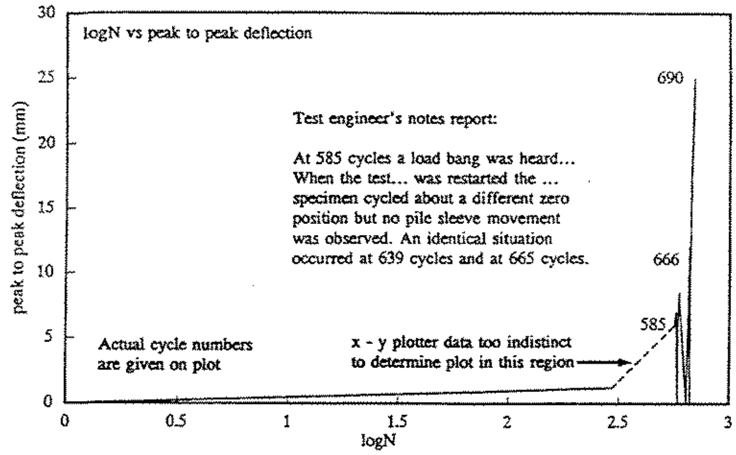

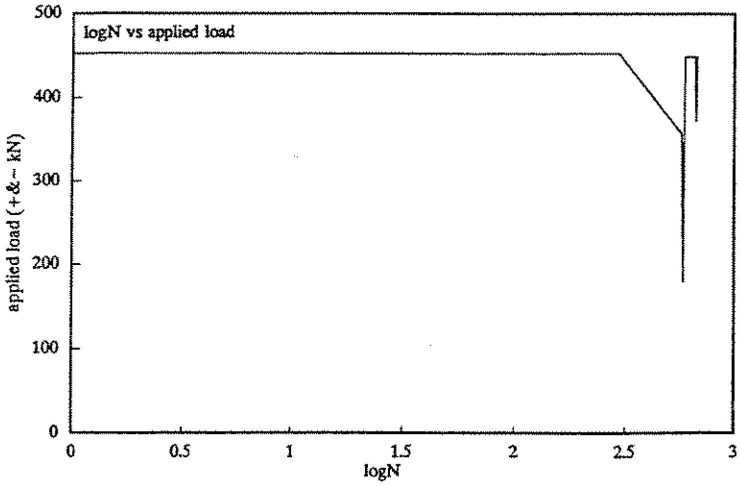

TEST NO 4 - 8

weld bead height to spacing ratio	h_{min}/s h_{av}/s	0.059 0.062
early age displacement	$\pm\ \delta/D$	0.0034
applied load / predicted static capacity	P/S	0.24
actual static capacity, post fatigue test	kN	-
equivalent estimated static capacity (without fatigue test)	kN	-
actual static capacity / equivalent predicted value		-
cycles to first 'failure'		690
final number of cycles achieved (R=runner)		690

Specimen was early age cycled with a foam seal retaining the grout. No grout leakage was actually recorded but the number of cycles recorded is possibly less than might have been achieved if there had been inflated seals.

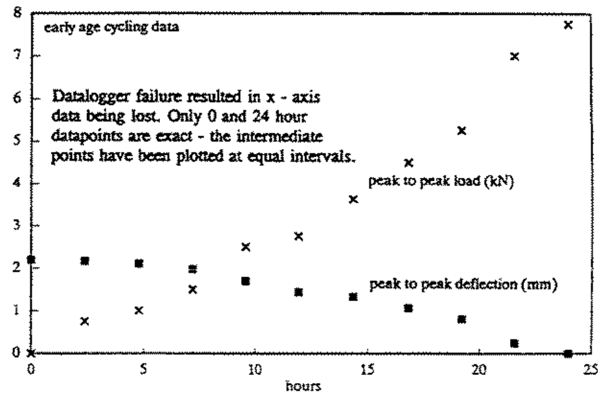

Frequency data not known except that at some time (after 294 cycles?) the frequency was reduced to 0.1 Hz (from 1.0 Hz?).

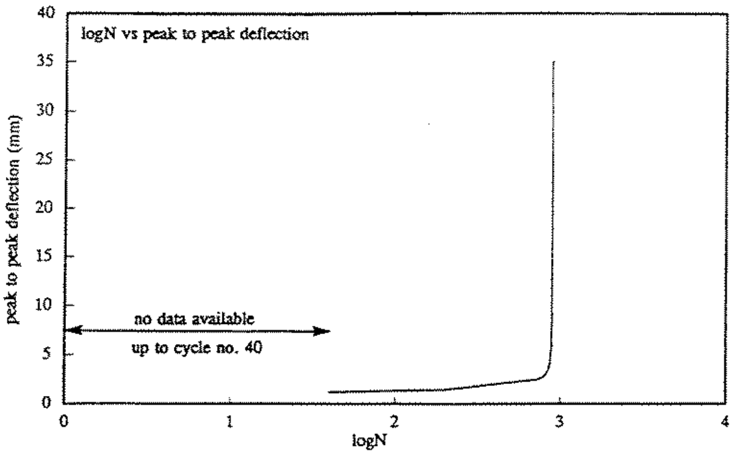

TEST NO 4 - 8.A

weld bead height to spacing ratio	h_{min}/s h_{av}/s	0.059 0.062
early age displacement	$\pm\ \delta/D$	0
applied load / predicted static capacity	P/S	0.48
actual static capacity, post fatigue test	kN	-
equivalent estimated static capacity (without fatigue test)	kN	-
actual static capacity / equivalent predicted value		-
cycles to first 'failure'		888
final number of cycles achieved (R=runner)		888

Although this specimen was grouted with a foam seal, it was not subjected to early age cycling and thus there is no reason to suspect the validity of the result.

Specimen loaded at ± 911kN and cycled at 0.1 Hz throughout the test.

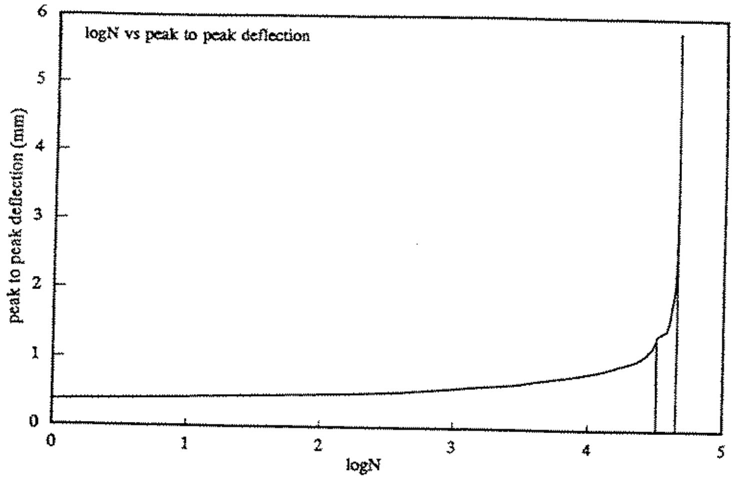

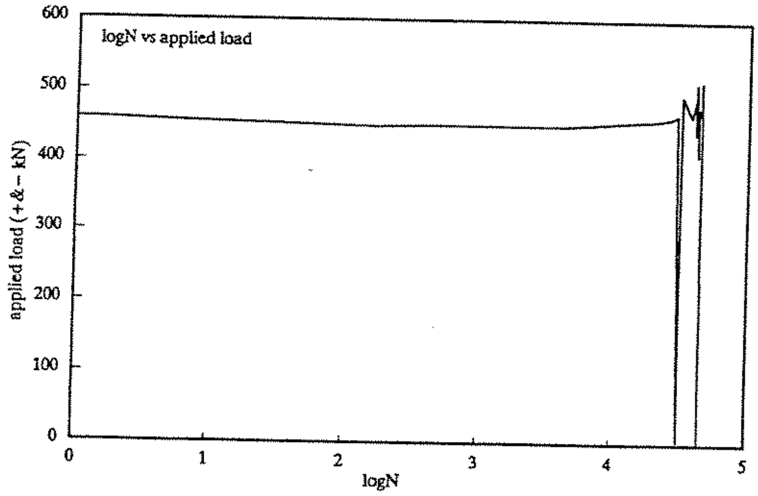

TEST NO 4 - 8.R

weld bead height to spacing ratio	h_{min}/s h_{av}/s	0.059 0.062
early age displacement	$\pm \delta/D$	0.0034
applied load / predicted static capacity	P/S	0.25
actual static capacity, post fatigue test	kN	-
equivalent estimated static capacity (without fatigue test)	kN	-
actual static capacity / equivalent predicted value		-
cycles to first 'failure'		44927
final number of cycles achieved (R=runner)		44927

Due to datalogger failure, the only early age cycling data that exists is that at zero hours the peak to peak deflection was 2.20mm and that at 24 hours the peak to peak load was 8.00 kN.

The only mention of frequency is that the specimen was set at 1.0 Hz. This statement was made by AEA Technology at 3712 & 31892 cycles. It is not known what it was cycling at immediately before these two values.

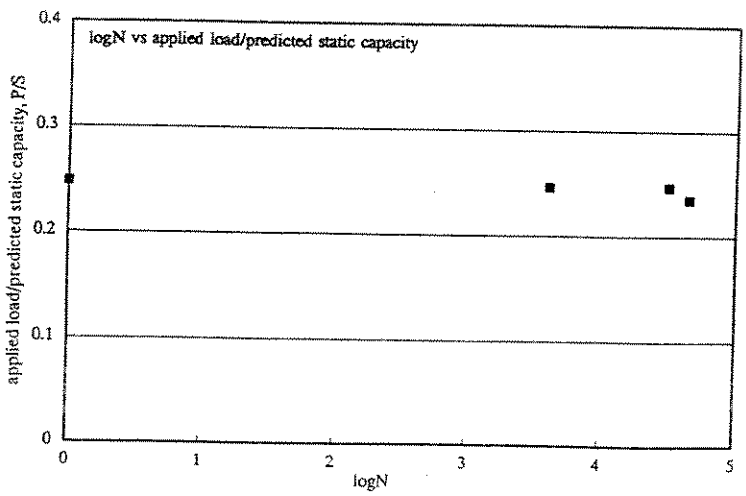

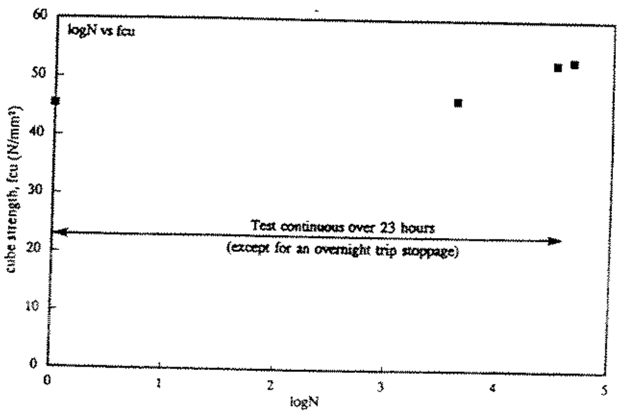

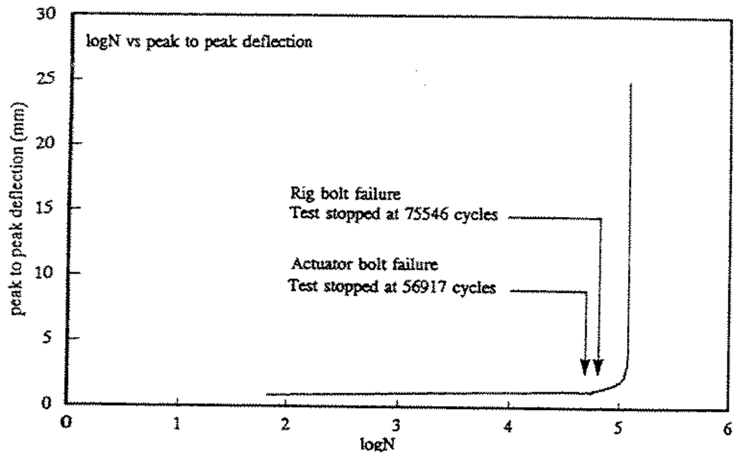

TEST NO 4 - 16

weld bead height to spacing ratio	h_{min}/s h_{av}/s	0.052 0.060
early age displacement	± δ/D	0
applied load / predicted static capacity	P/S	0.23
actual static capacity, post fatigue test	kN	430
equivalent estimated static capacity (without fatigue test)	kN	2382
actual static capacity / equivalent predicted value		0.18
cycles to first 'failure'		120030
final number of cycles achieved (R=runner)		120030

During early age cycling, the pile remained static whilst the sleeve was moved.

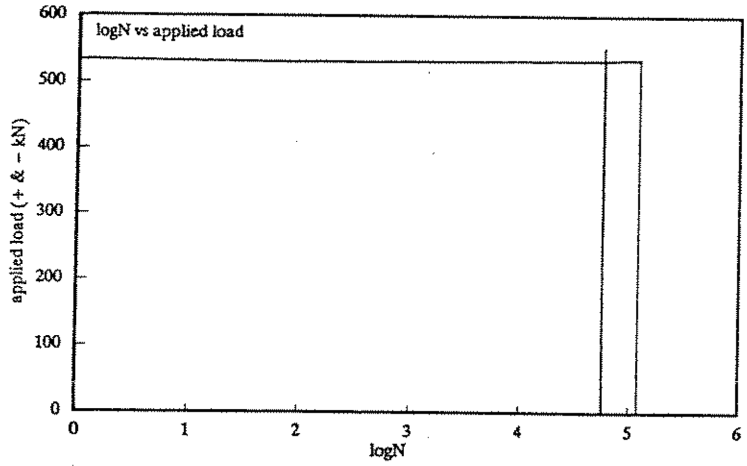

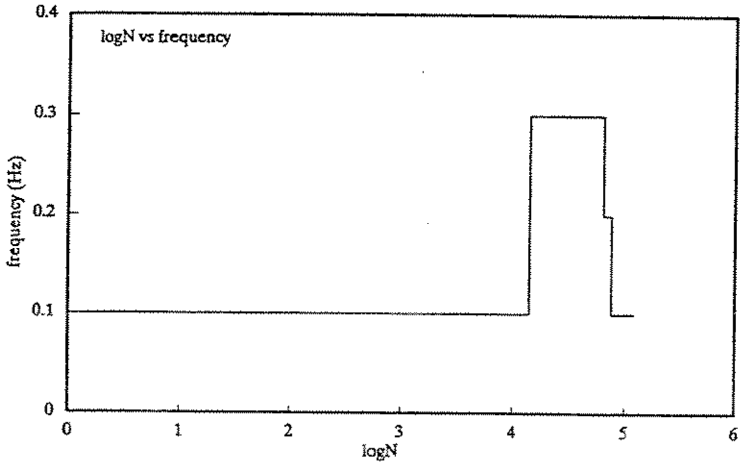

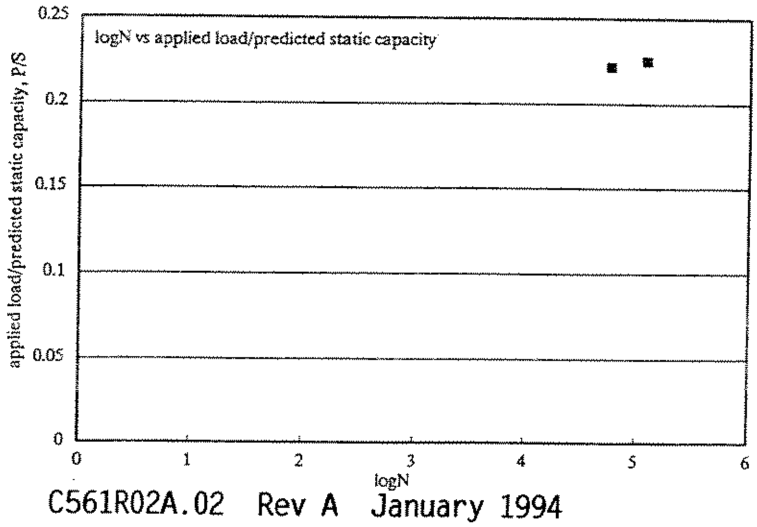

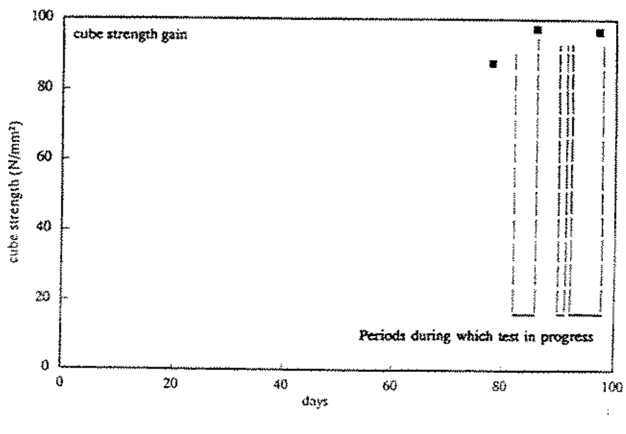

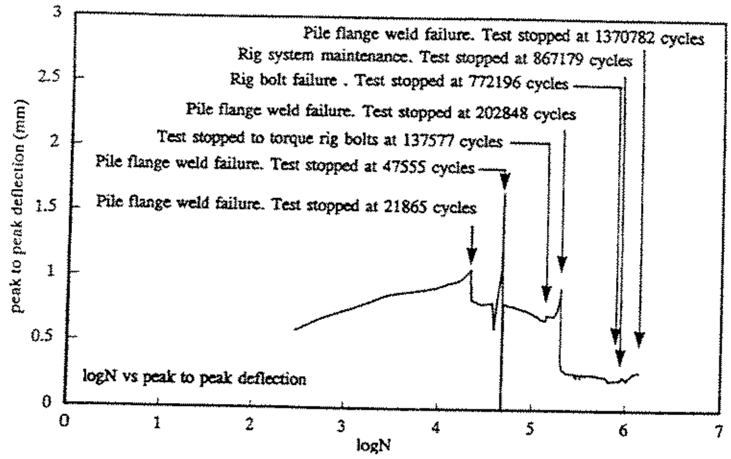

TEST NO 4 - 17

weld bead height to spacing ratio	h_{min}/s h_{av}/s	0.059 0.062
early age displacement	± δ/D	0
applied load / predicted static capacity	P/S	0.21
actual static capacity, post fatigue test	kN	> 1938*
equivalent estimated static capacity (without fatigue test)	kN	2462
actual static capacity / equivalent predicted value		> 0.79*
cycles to first 'failure'		
final number of cycles achieved (R=runner)		1370782 R

* Test machine capacity reached at 1938kN.

During early age cycling, the pile remained static whilst the sleeve was moved.

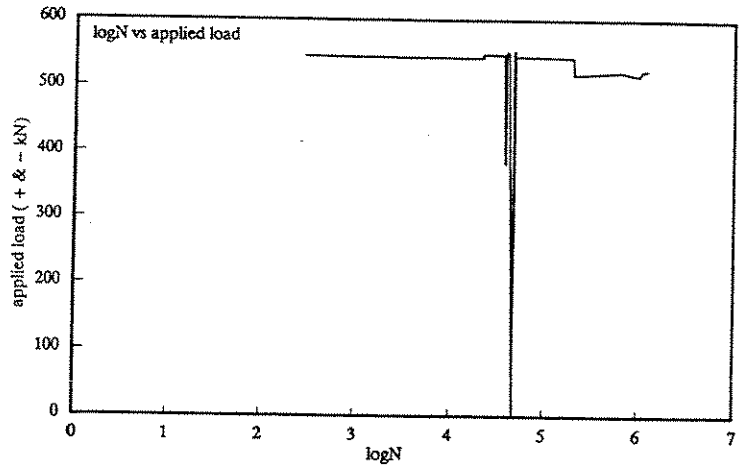

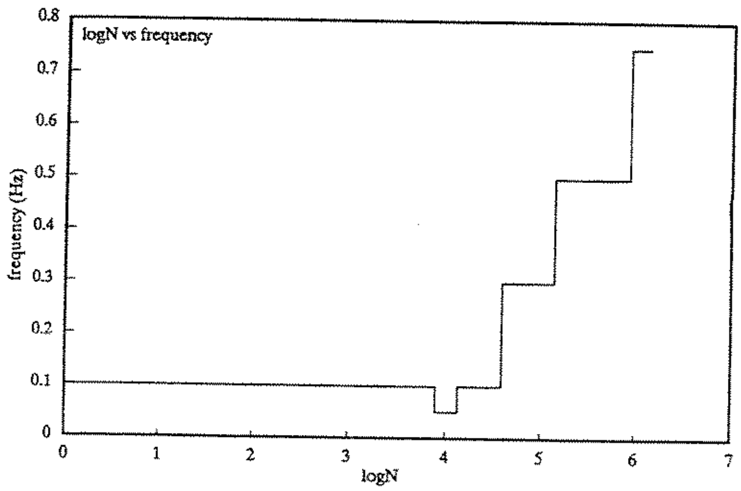

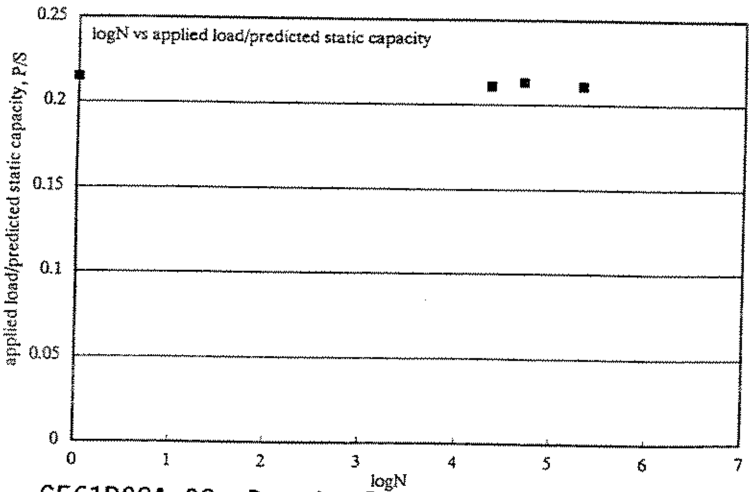

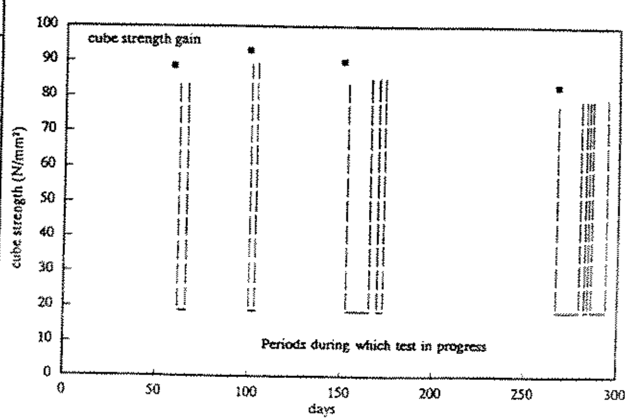

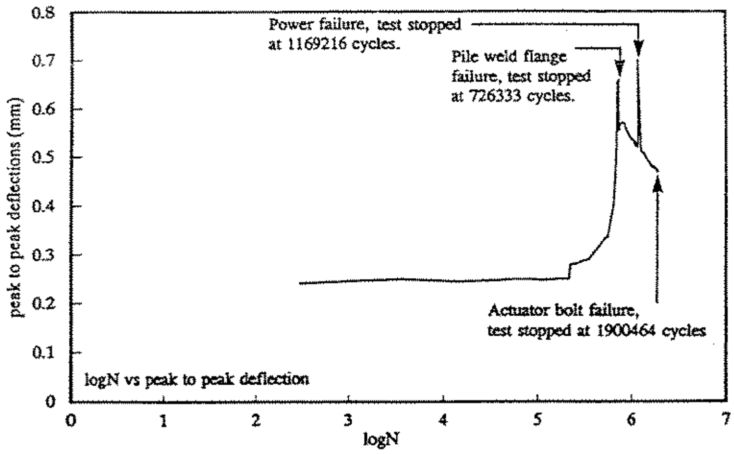

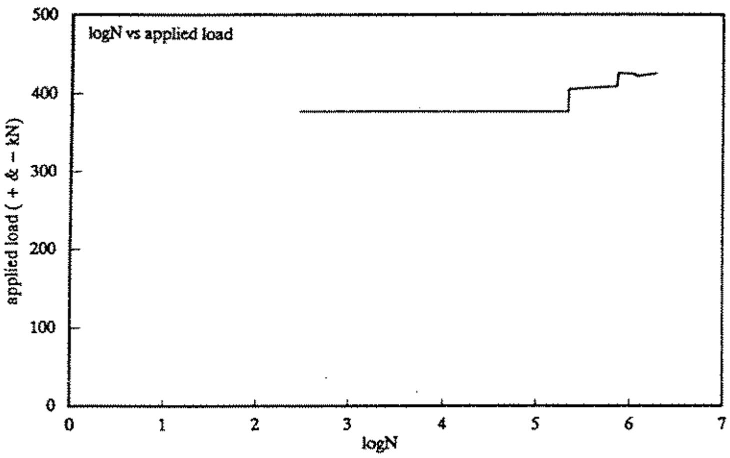

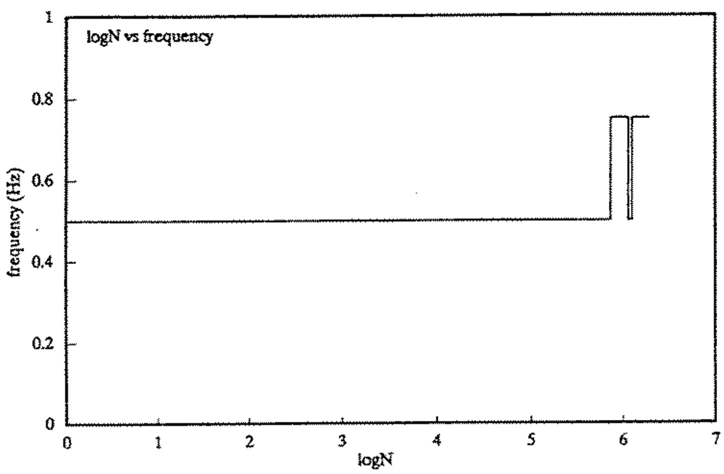

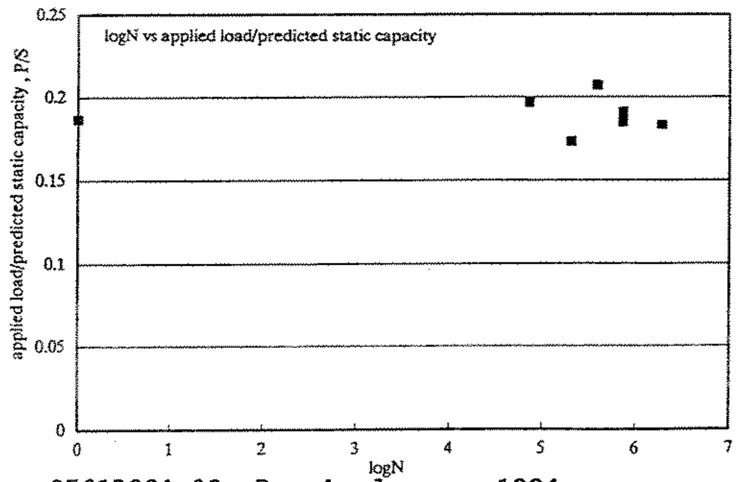

TEST NO 4 - 18

weld bead height to spacing ratio	h_{min}/s h_{av}/s	0.052 0.060
early age displacement	± δ/D	0
applied load / predicted static capacity	P/S	0.19
actual static capacity, post fatigue test	kN	-
equivalent estimated static capacity (without fatigue test)	kN	-
actual static capacity / equivalent predicted value		-
cycles to first 'failure'		-
final number of cycles achieved (R=runner)		1900464 R

During early age cycling, the pile remained static whilst the sleeve was moved.

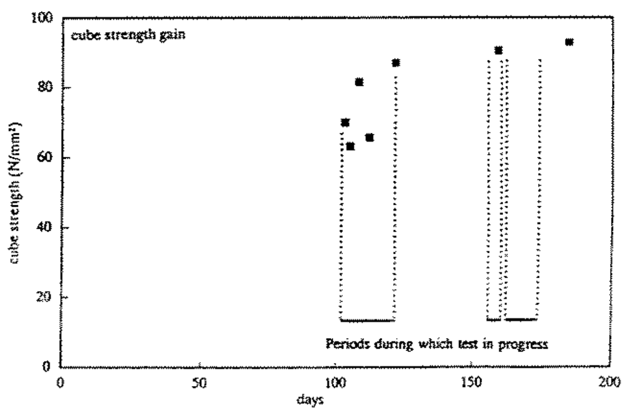

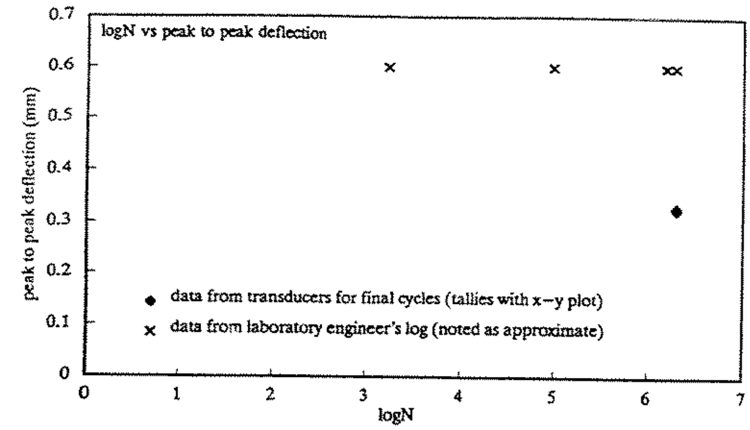

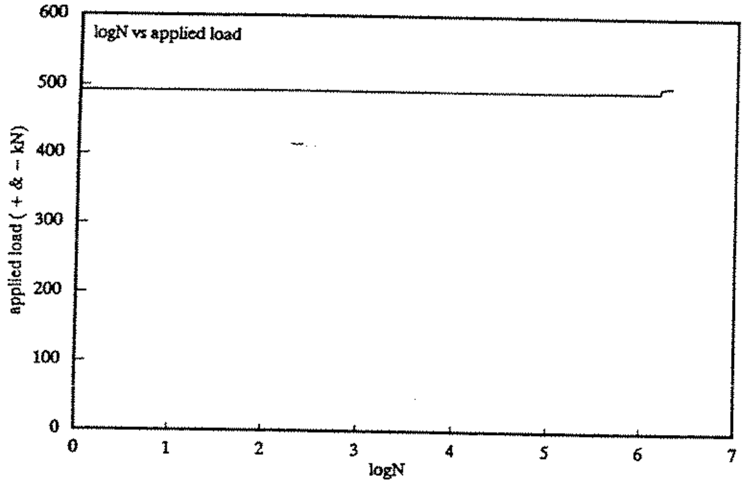

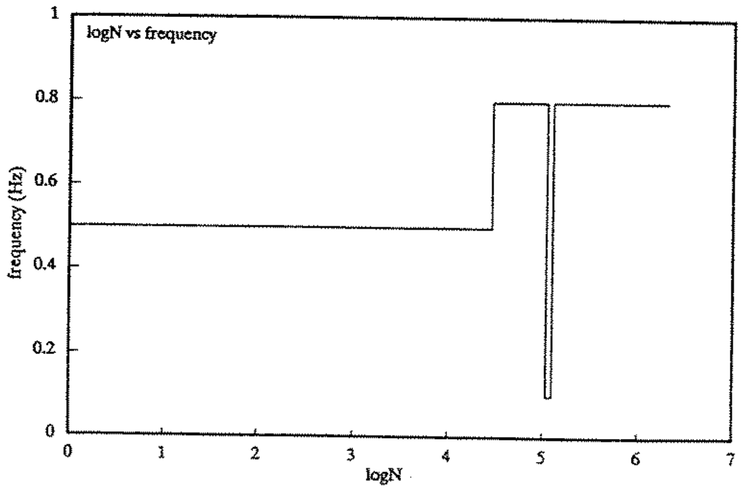

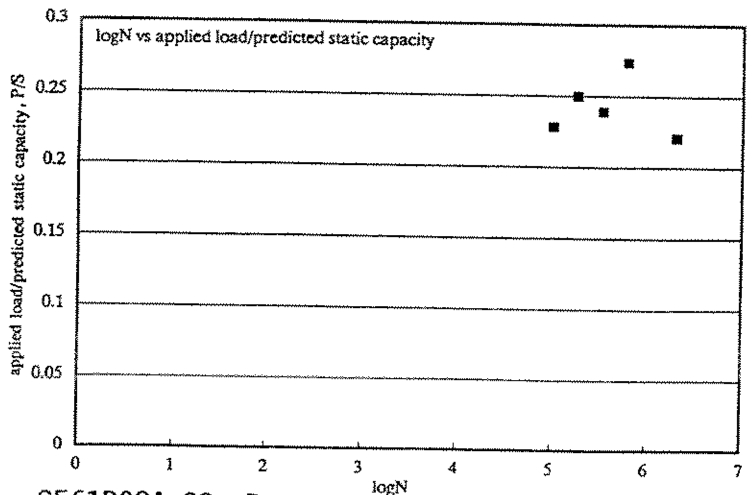

TEST NO 4 - 19

weld bead height to spacing ratio	h_{min}/s h_{av}/s	0.058 0.060
early age displacement	$\pm\ \delta/D$	0
applied load / predicted static capacity	P/S	0.24
actual static capacity, post fatigue test	kN	> 1959*
equivalent estimated static capacity (without fatigue test)	kN	2275
actual static capacity / equivalent predicted value		> 0.86*
cycles to first 'failure'		-
final number of cycles achieved (R=runner)		2006864 R

* Test machine capacity reached at 1959kN. Specimen was still behaving linearly at this point.

During early age cycling, the pile remained static whilst the sleeve was moved.

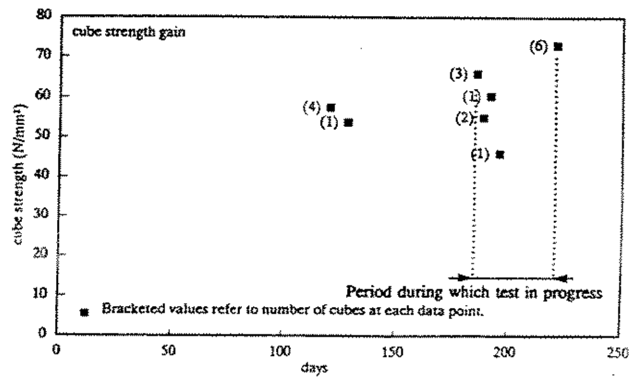

6 EVALUATION OF THE TEST RESULTS:

6.1 Specimen no 1

Due to the limited capacity of the steel sections it is not possible to test specimens with high length to diameter ratios. With an L/D ratio of 1.25 and $S/\sqrt{RT}$ ratio of 6 only two shear keys can be accommodated. This gives rise to significant end effects associated with the length of grout which is outside the shear keys and thus not confined. The static strength of specimen no 1 is controlled by the strength of the grout matrix. For this failure mode we have limited information and there is uncertainty associated with the ultimate strength.

Due to the above uncertainties which are found to have a significant impact it has been found relevant to plot this test as a range as shown in Fig. 6.1.1.

6.2 Specimen no 3

Due to the uncertainty associated with the reference static strength of specimen no 1 a static strength test was run for specimens with a $S/\sqrt{RT}$ ratio of 1.

6.3 Plain fatigue tests

The plain fatigue test include the following

DnV - Tests:

-	Specimen no 1	plotted as a range
-	Specimen no 2	1200 kN plotted as 38%
-	Specimen no 5	plotted as 20%

UK - Tests:
Test no. 4 - 8A
Test no. 4 - 16
Test no. 4 - 17
Test no. 4 - 18
Test no. 4 - 19

4 August 1994, T&I-212 O:\BGF\161119\94-3243.REP

In addition specimen 8 is recorded as a lower bound to plain fatigue. The results are plotted in Fig. 6.3.1 in terms of the dynamic to static load ratio versus the logarithm of the number of cycles. In Fig. 6.3.2 the log of the load ratio is plotted against Log N.

The above data is limited, but it seems clear that there is a reduced fatigue capacity relative to static strength when heavier shear keys are introduced. Very tentatively it is proposed that this trend is something of the order of:

$$\frac{F_{cmax}}{F_{cu}} = 10^{\left(-\sqrt{10h/s} - 0.06\, Log n\right)}$$

4 August 1994, T&I-212 O:\BGF\161119\94-3243.REP

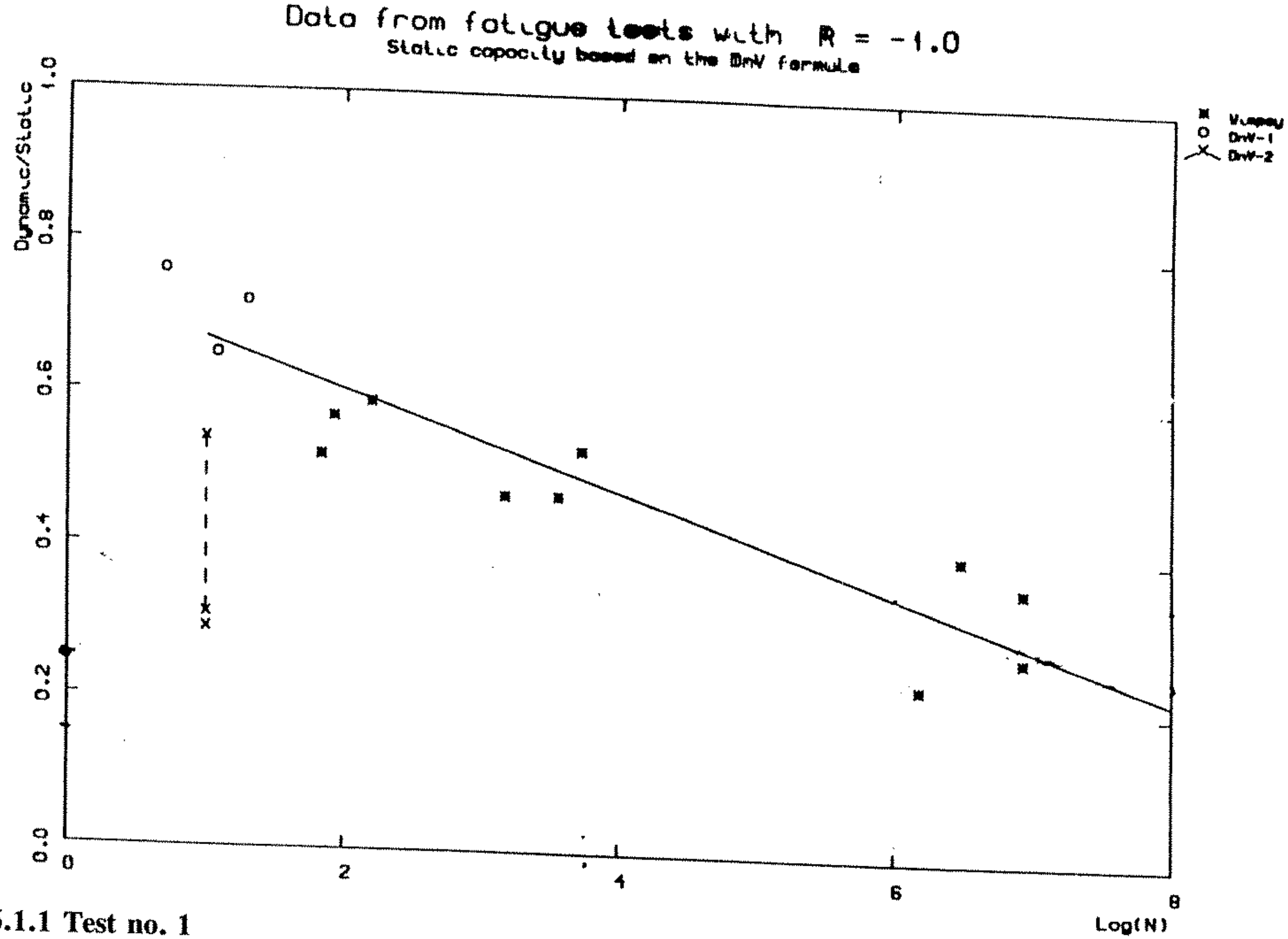

Figure 6.1.1 Test no. 1

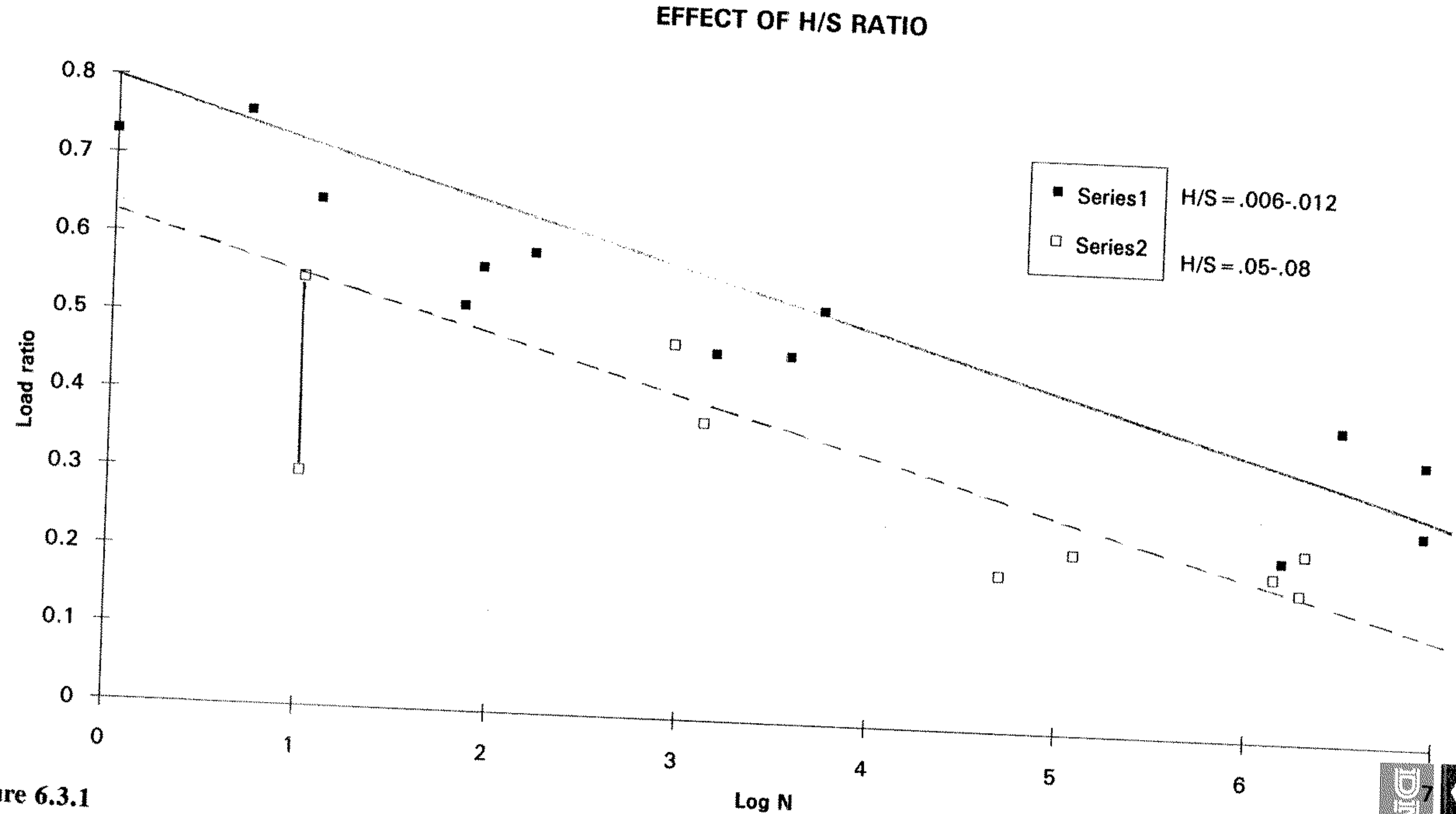
EFFECT OF H/S RATIO
0.8
0.7
0.6
0.5
0.4
0.3
0.2
0.1
0
Load ratio
0
1
2
3
4
5
6
7
Log N
Series1 H/S = .006-.012
Series2 H/S = .05-.08

Figure 6.3.1

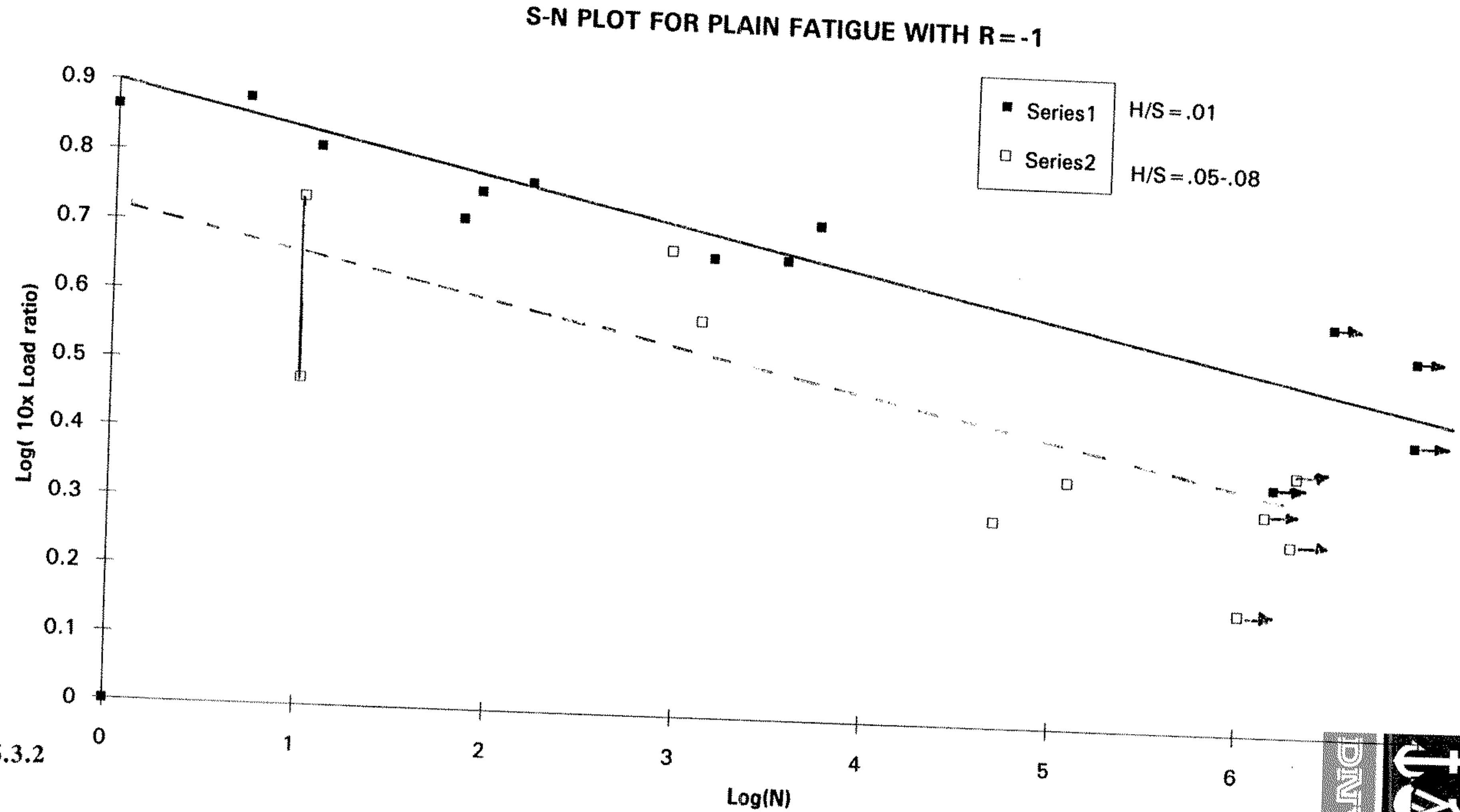
S-N PLOT FOR PLAIN FATIGUE WITH R=-1
Series1
H/S=.01
Series2
H/S=.05-.08
0.9
0.8
0.7
0.6
0.5
0.4
0.3
0.2
0.1
0
Log(10x Load ratio)
0
1
2
3
4
5
6
Log(N)

Figure 6.3.2

6.4 Tests with early age cycling and fatigue

The tests with early age cycling followed by fatigue testing include the following specimens:

- Specimen no 4 - 600 kN amplitude plotted as 19%
- Specimen no 7 - 600 kN amplitude plotted as 21%
- Specimen no 8 - 650/800 kN amplitude plotted as 22%
- Specimen no 9 - 650 kN amplitude plotted as 20%
- Test no 4 - 7 - 880 kN amplitude plotted as 39%
- Test no 4 - 8 - 460 kN amplitude plotted as 24%
- Test no 4 - 8R - 470 kN amplitude plotted as 25%

These test results have been plotted in fig. 6.4.1. In this figure the average trend for plain fatigue tests with high shear key upstand to pitch ratio from fig. 6.3.1 has also been plotted as a reference.

All the DNV specimens have been tested with a fatigue load amplitude of approximately 20% of their static strength. These are marked with their specimen number. Specimen no 4 is the basic reference case. This specimen has a shear key spacing ratio $S/\sqrt{RT}$ of 1 and has been subjected to an early age cycling displacement of 1 mm. It shows very considerable impact from early age cycling.

Specimen no 7 is identical to specimen no 4, but was subjected to an early age cyclic displacement of only 0.3 mm. The reduced disturbance has significantly improved the performance.

Specimens nos. 8 and 9 are nominally identical. They both have a shear key spacing ratio $S/\sqrt{RT}$ of 3 which is three times larger than that of specimen no. 4. Otherwise they are identical to specimen no 4. They show a radically improved performance. They more or less fall within the scatter band of the test run without early age cycling.

There is also a very significant difference between the performance of specimens 8 and 9. Test observations indicate that this is related to the impacting effect of running the actuator in force control. Fatigue tests are conventionally run in force control in order to maintain a constant force amplitude under increasing displacement amplitude. If this is an important effect it will have had a greater impact on specimen no 9 than on specimen no 8. It will also potentially have had an impact on all tests performed so far. Future tests must be run with a modified force control which limited the displacement rate to a level representative of that which would be experienced in an offshore structure.

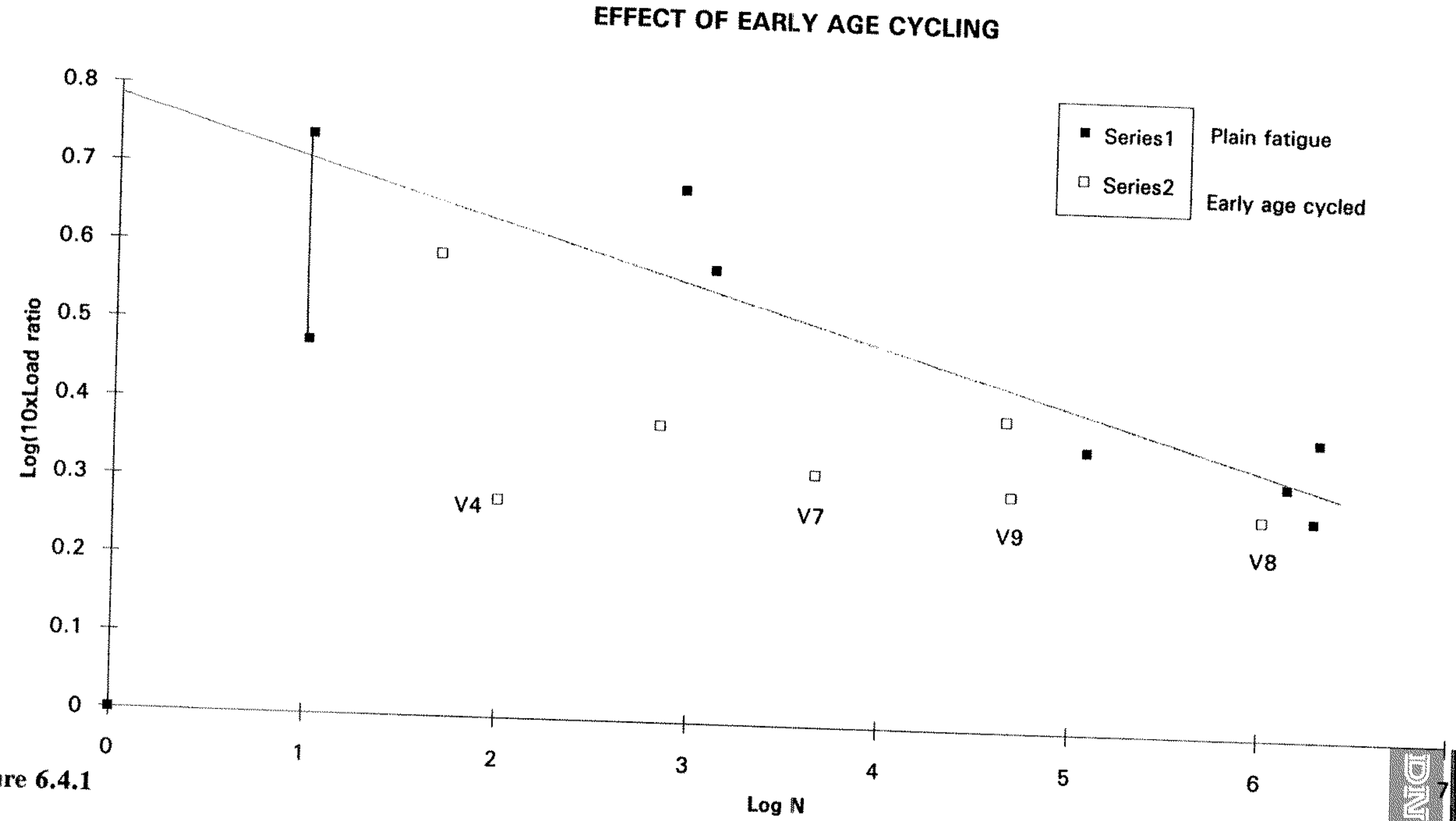
EFFECT OF EARLY AGE CYCLING
0.8
0.7
0.6
0.5
0.4
0.3
0.2
0.1
0
Log(10xLoad ratio
0
1
2
3
4
5
6
7
Log N
Series1
Series2
Plain fatigue
Early age cycled
V4
V7
V9
V8

Figure 6.4.1

The UK specimens are observed to be less influenced by early age cycling and to show a less consistent trend.

6.5 Tests with early age cycling only

Specimens nos 6 and 10 were both exposed to early age cycling with a displacement of 1 mm. They differ in that specimen no 6 has a shear key spacing ratio S/√RT or 1 while specimen no 10 has a shear spacing ration of 3. Both specimens have been sectioned after the early age cycling exposure. In both cases a very narrow zone of disturbed grout has been identified. In specimen no 6 this zone forms a straight line through the specimen and accounts for the reduced performance due to early age cycling.

In specimen no 10 the disturbed zone angled out from the top of the shear keys towards the grout to steel interface and followed this up to a point where it deflected out to rise above the next shear key. This undulating shape of the disturbed zone allows the wedging action of the shear keys to be mobilized and accounts for the greatly enhanced performance of specimens nos. 8 and 9 in the early age cycling tests with fatigue.

7 REFERENCES

/1/ VERITEC report no. 92-3200, "Recommendations for rule and code provisions for the design of grouted connections"

/2/ VERITEC report no. 90-3864, "Report on screening of data base on test results"

/3/ VERITEC report no. 91-3442, "Report on Code Calibration"

/4/ VERITEC report no. 92-3192, "Report on Formulae Fitting and Code Calibration"

/5/ VERITEC report no. 91-3446, "Tests of interface friction between grout and steel"

/6/ VERITEC report no. 92-3199, "Two axial Compression Tests on Grouted Pile Sleeve Connections"

/7/ Billington, C.J. and Tebett I.E., Wimpey Laboratories Ltd. "Fatigue Strength of Grouted Tubular Steel Connections for Offshore Structures." International Association for Bridge and Structural Engineering (IABSE), Lausanne, 1982.

/8/ VERITEC report no. 84-3073, "Grouted Pile-Sleeve Connections in Steel Platforms". part Project 4, Dynamic Testing of Shear Key Specimens.

/9/ UK Department of Energy: "A study of length Longitudinal Stiffening and Size Effects on Grouted Pile - Sleeve Connections". OTH 86 230, 1987.

/10/ BP International Ltd. Report C561RO2A.02, Rev. A: "Joint Industry Project Grouted Pile-Sleeve Connections; Factual Report on Test Series 4", January 1994.

APPENDIX A

SPECIFICATION OF OIL WELL G CEMENT

84-3072
VT/67/R3

D.1 DNV

NORWELL API CLASS G CEMENT FOR CONCRETE.

CHEMICAL COMPOSITION.

MgO	App.:	1.85 %	(6.00 %	Max.)
SO_3	" :	1.90 %	(3.00 %	Max.)
Loss on Ignition	" :	0.45 %	(3.00 %	Max.)
Insoluble Residue	" :	0.20 %	(0.75 %	Max.)
3 CaO. SiO_2	" :	61.0 %	(65.0 %	Max.)
			(48.0 %	Min.)
3 CaO.Al_2O_3	"	0.9 %	(3.0 %	Max.)
4 CaO. Al_2O_3. Fe_2O_3+ 2.3 CaO.Al_2O_3	" :	17.3 %	(24.0 %	Max.)
Total Alkali Na_2O equivalent		0.62 %	(0.75 %	Max.)

The cement is HIGH RESISTANT (HSR)

Concrete Cube Strength vs W/C-ratio.

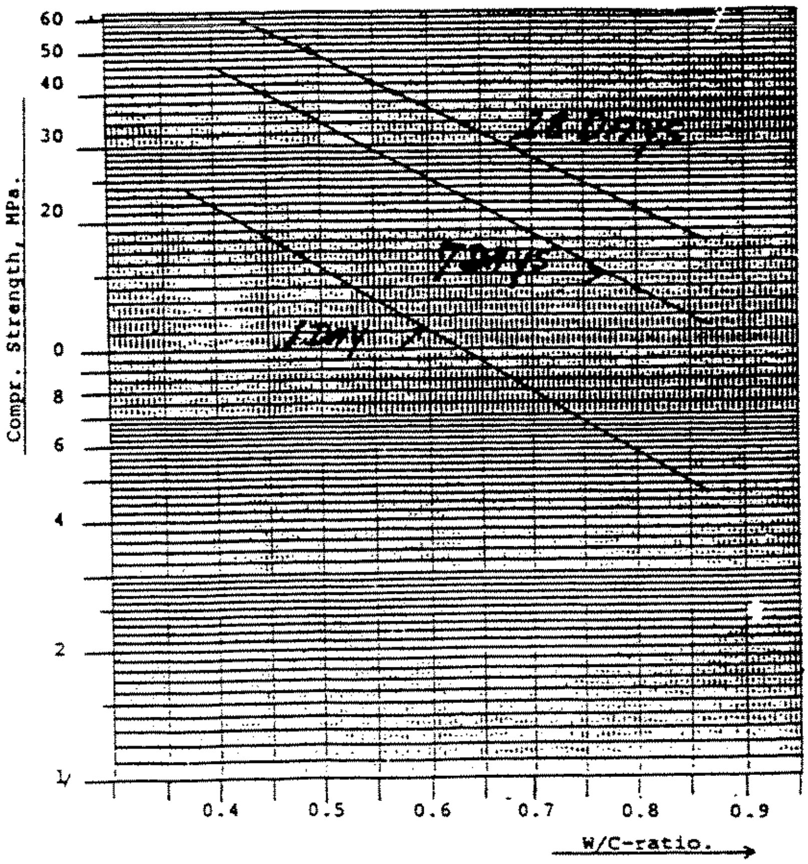

The substitute sea water was mixed in accordance with DIN 50906 and the compounds in each dm^3 of sea water were:

NaCl	28.0 gr.
$MgCl_2$	5.0 gr.
$CaCl_2$	2.4 gr.
$NaHCO_3$	0.2 gr.
$MgSo_4$	7.0 gr.

The density of this substitute water was 1.0235 kg/dm^3.